INSULIN MEDIATED REGULATION OF SARCOMERIC PROTEIN EXPRESSION

Dissertation

zur Erlangung des akademischen Grades
doctor medicinae (Dr. med.)

vorgelegt dem Rat der Medizinischen Fakultät
der Friedrich-Schiller-Universität Jena

von Katharina Gerda Maria Heinrich
geboren am 12.05.1993 in Hamburg

Gutachter:

1. **Prof. Dr. med. Torsten Doenst**
   Klinik für Herz- und Thoraxchirurgie, Universitätsklinikum Jena

2. **Prof. Dr. med. Marcus Franz**
   Klinik für Innere Medizin I, Universitätsklinikum Jena

3. **PD Dr. med. Heiko Bugger**
   Klinik für Kardiologie und Angiologie I, Universitäts-Herzzentrum Freiburg

Tag der öffentlichen Verteidigung: 17.04.2018
Tag des Staatsexamens: 11.12.2018

Table of contents

1 List of abbreviations

A	alpha
°C	degree Celsius
µg	microgram
µl	microliter
µM	micromolar
Acta1	skeletal muscle alpha actin
Acta2	smooth-muscle alpha actin
Akt	protein kinase B
ANP	atrial natriuretic peptide
BNP	brain natriuretic peptide
cDNA	complementary deoxyribonucleic acid
CHO-IR	Chinese hamster ovary cells overexpress human insulin receptor
cIR-IGFRdKO	mice with cardiac inducible knockout of insulin receptor and insulin-like growth factor 1 receptor
cIRSdKO	mice with cardiac inducible knockout of insulin receptor substrate 1 and 2
Cops6	COP9 signalosome complex subunit 6
dKO	double knockout (cIR-IGFRdKO and cIRSdKO) mice
DMSO	dimethylsulfoxide
DNA	deoxyribonucleic acid
ERK	extracellular signal-regulated kinases
g	gram
GAPDH	glyceraldehyde 3-phosphate dehydrogenase
Gja1	gap junction protein
IGF	insulin-like growth factor-1
kb	kilobase pairs
kg	kilogram
KO	cIR-IGFRdKO knockout mice
M	molar
MAPK	mitogen activated protein kinases
mg	milligram
min	minute

ml	milliliter
mm	millimeter
mM	milimolar
mRNA	messenger ribonucleic acid
Myh7	cardiac beta myosin heavy chain
Myocd	myocardin
ng	nanogram
nM	nanomolar
NRCM	neonatal rat cardiomyocytes
p90RSK	phosphorylated 90 kDa ribosomal S6 kinase
Pdlim5	PDZ and LIM Domain 5
PI3K	phosphatidylinositol 3-kinase
PMA	phorbol 12-myristate 13-acetate
qPCR	quantitative polymerase chain reaction
RSK	ribosomal s6 kinase
sec	second
SRE	serum response element
SRF	serum response factor
Tnni1	slow skeletal muscle troponin I
Tnnt2	cardiac muscle troponin T
Trim63	tripartite motif containing 63
WT	cIR-IGFRdKO wildtype mice

2 Zusammenfassung

Sowohl Insulin als auch Insulin-like growth factor 1 (IGF) aktivieren vielfältige Signalkaskaden im Herzen, die für einen ausreichenden Stoffwechsel und eine gute Funktion unerlässlich sind. Die Signale regeln unter anderem Kontraktilität, Metabolismus, Hypertrophie und Autophagie der Herzmuskelzellen. Um die Auswirkungen einer ausgeschalteten Insulin und IGF Signalkaskade im Herzen zu untersuchen, wurden Mäuse mit induzierbarer, kardialer Null-Mutation verwendet. In einem Mausmodell wurde der Insulinrezeptor und IGF-Rezeptor ausgeschaltet, in einem anderen die Insulin-Rezeptor-Substrate 1 und 2. Beide Mausmodelle (dKO) wiesen einen ähnlichen Phänotyp, der mit Herzinsuffizienz und erhöhter Mortalität assoziiert war, auf. In den Mausmodellen wurden eine veränderte Sarkomerstruktur und eine Herunterregulation von an der Herzstruktur beteiligten Genen gefunden. Es ist noch nicht abschließend geklärt, wie Insulin die Expression von Sarkomerproteinen beeinflusst und somit die kontraktile Funktion des Herzens aufrechterhält.

Ziel dieser Arbeit war es, die Rolle der Insulin Signalkaskade bei der Regulation der Expression von Sarkomerproteinen zu untersuchen.

Neonatale Ratten Kardiomyozyten (NRCM) wurden aus Wistar Ratten isoliert. Die NRCM wurden für 1 Stunde mit PD98059, einem ERK-Phosphorylierungsinhibitor, vorbehandelt und für 4, 24 oder 48 Stunden mit Insulin stimuliert. mRNA wurde isoliert und mit Hilfe von qPCR quantifiziert.
Chinese Hamster Ovary Zellen mit Überexpression des Insulinrezeptors wurden mit einem Reportergenkonstrukt, das entweder Skelettmuskel alpha Actin (Acta1) oder glatte Muskel alpha Actin (Acta2) Promoter enthält, transfiziert. Anschließend wurden die Zellen für 24 Stunden mit Insulin stimuliert und die Transkriptionsaktivität gemessen.
In 8 Wochen alten, transgenen Mäusen wurde die kardiale Expression von Insulinrezeptor und IGF-Rezeptor ausgeschaltet. Eine Woche nach der Genausschaltung wurden die weiblichen und männlichen Mäuse mit Insulin stimuliert. Die Proteinexpression wurde mit Hilfe von Western Blots analysiert.

Herzen aus Mäusen mit gleichzeitiger Null-Mutation (KO) des Insulinrezeptors und IGF-Rezeptors wogen 15% weniger als Wildtyp (WT) Herzen. Außerdem war das Verhältnis vom Herzgewicht zum Körpergewicht in WT Mäusen im Vergleich zu KO Mäusen signifikant höher. Die kardiale Proteinexpression von Insulinrezeptor und IGF-Rezeptor war in KO

Mäusen reduziert. Insulinstimulation führte zu einer Phosphorylierung von Akt, die in KO Herzen weniger ausgeprägt war als in WT Herzen. Eine vorausgegangene Expressionsanalyse ergab, dass mehrere für Sarkomerproteine codierende mRNAs in dKO Mäusen herunterreguliert waren.
Insulinstimulation der NRCM führte zu einem signifikanten Anstieg der Menge an Acta1 und Acta2 mRNA. ERK-Hemmung in den NRCM verhinderte die Phosphorylierung von ERK und RSK durch Insulinstimulation und hemmt möglicherweise die durch Insulin induzierte Acta1 und Acta2 mRNA Expression.
Ein unabhängiger Ansatz zur Überprüfung der Signalkaskade wurde unter Verwendung eines Zellkulturmodells und transkriptionellen Reporterkonstrukten angestrebt, um zu bestimmen, ob die Signalkaskade von Insulin den serum response factor (SRF) aktiviert und somit die Expression der Sarkomerproteine kontrolliert. Insulin hatte hier keine spezifische Wirkung auf die Acta1 und Acta2 Promotoraktivitäten. Das Ausmaß der Aktivierung von Acta1 und Acta2 Promotoren durch die Insulinstimulation war ähnlich des eines Luciferaseplasmides mit einem minimalen Promotor. Transfektionen ohne Myocardin, einem Coaktivator von SRF, führten zu niedrigeren Promotoraktivitäten.

Zusammenfassend betrachtet scheint die Insulinstimulation keine spezifische Wirkung auf die Acta1 und Acta2 Promotoraktivitäten durch einen SRF abhängigen Mechanismus zu haben. Allerdings deuten unsere Daten der mRNA Expression in NRCM darauf hin, dass Insulin eine Wirkung auf die Acta1 und Acta2 Expression hat. Ob dieser Effekt direkt oder indirekt ist, muss noch abschließend geklärt werden.

3 Abstract

Insulin signaling and insulin-like growth factor-1 (IGF) signaling display pleiotropic effects in the heart, which are required for normal cardiac metabolism and function. Signal transduction regulates amongst others: contractility, metabolism, hypertrophy, and autophagy. To study the effects of a loss of insulin and IGF signaling in the adult heart, mice with cardiac inducible double knockout (dKO) of insulin receptor and IGF receptor or insulin receptor substrates 1 and 2 have been generated previously. Both models display overlapping phenotypes with heart failure and increased mortality. dKO mice show sarcomeric disarray and downregulation of genes involved in cardiac structure. It is incompletely understood, how insulin signaling preserves contractile function by maintaining sarcomeric protein expression.

The aim of the current study was to investigate the role of insulin signaling in the regulation of sarcomeric protein expression.

Neonatal rat cardiomyocytes (NRCM) were isolated from Wistar rats and stimulated with insulin for 4, 24 or 48 hours. Furthermore, NRCM were pretreated for 1 hour with PD98059, an ERK phosphorylation inhibitor, and stimulated for 24 hours with insulin. mRNA was purified and quantified with qPCR.
Chinese hamster ovary cells with overexpression of insulin receptor were transfected with reporter constructs containing skeletal muscle alpha actin (Acta1) or smooth-muscle alpha actin (Acta2) promoters. Cells were then treated with vehicle or insulin for 24 hours and transcriptional activity was monitored.
A cardiomyocyte-restricted and doxycycline-inducible Cre expressing transgene was used to delete the insulin receptor and IGF receptor in 8-week-old mice. One week after knockout induction mice were stimulated with insulin or saline. Protein expression was analyzed with western blots.

Hearts from mice lacking insulin receptor and IGF receptor (KO) weighed 15% less than wildtype (WT) hearts and the heart to body weight ratios were significantly higher in WT compared to KO mice in both sexes. Cardiac insulin receptor and IGF receptor protein expression was reduced in KO mice. Insulin stimulation led to Akt phosphorylation in the heart, which was partly reduced in KO. Previously, expression profiling revealed that several mRNAs coding for sarcomeric proteins were downregulated in dKO mice.

Insulin stimulation in NRCM led to a significant increase in Acta1 and Acta2 mRNA expression levels. ERK inhibition in NRCM prevented ERK and RSK phosphorylation after insulin stimulation, and may inhibit insulin induced Acta1 and Acta2 expression.
To assess the signaling in an independent approach, a cell culture model and transcriptional reporter constructs were utilized to determine whether insulin signaling actives serum response factor (SRF) activity to control sarcomeric protein expression. Insulin stimulation did not show a specific effect on Acta1 and Acta2 promoter activities. The magnitude of Acta1 and, Acta2 promoter activity after insulin stimulation was similar to that of a luciferase plasmid with a minimal promoter. Transfections without myocardin, a coactivator of SRF, led to lower promoter activities.

In conclusion, insulin stimulation does not seem to show a specific effect on Acta1 and Acta2 promoter activities through an SRF dependent mechanism. However, our NRCM mRNA expression data suggests that insulin has an effect on Acta1 and Acta2 expression. Whether this effect is direct, or indirect, remains to be definitively determined.

4 Introduction

Cardiovascular diseases are the leading causes of death in Germany. Approximately 40% of all deaths are caused by chronic ischemic heart disease, acute myocardial infarction and heart failure (Statistisches Bundesamt 2015). Heart failure is defined as the failure of the heart to adequately supply the body periphery with blood. The heart cannot ensure tissue supply with oxygen and substrates. Multiple heterogeneous pathophysiological mechanism were described as causes for heart failure (MacIver et al. 2013).

One of the suggested mechanisms is a change in metabolism and signaling pathways caused by insulin resistance (Riehle und Abel 2016). Insulin resistance is a pathological condition in which cells are less sensitive to insulin stimulation than healthy cells. Insulin resistance is the most powerful predictor of future development of type 2 diabetes mellitus (Taylor 2012). Diabetes mellitus is associated with an increased risk of heart failure (Kannel et al. 1974) and the severity of insulin resistance correlates with the severity of heart failure (Swan et al. 1997). Furthermore, diabetic patients with cardiovascular disease present higher morbidity and mortality than nondiabetic patients (Mytas et al. 2009). It has been suggested, that insulin-regulated transcription factors might be involved in the development of cardiovascular diseases (Muller-Wieland et al. 2001).

4.1 Insulin and insulin signaling

Langerhans cells from the pancreas produce proinsulin, which is processed in the Golgi apparatus by proteolytic cleavage to insulin. Cells secrete insulin based on the blood glucose level (Rassow et al. 2008). The main effect of insulin is the regulation of glucose metabolism in different cells. Liver, muscle and adipose tissue are the most sensitive organs to insulin. Furthermore, insulin plays a role in protein metabolism and cell growth, stimulating uptake of amino acids into cells and increasing protein biosynthesis (Dimitriadis et al. 2011). Besides its fast metabolic effects, insulin has long term effects on transcriptional activity. Several genes have been shown with insulin sensitive elements on their promoter regions. For a subset, insulin reduces transcription. For others, insulin enhances transcription (Mounier und Posner 2006). Insulin influences the regulation of more than 150 genes (O'Brien et al. 2001). This regulation is not completely understood.

Insulin acts on its receptor, which belongs to the receptor tyrosine kinase family. Insulin receptor contains two extracellularly located alpha subunits and two membrane-spanning beta

subunits with tyrosine kinase activity. Binding of insulin promotes autophosphorylation and activates regulation of target proteins. Important phosphorylation targets are insulin receptor substrates 1 and 2 (Lee und Pilch 1994).

Binding of insulin to its receptor activates two main pathways. On the one hand binding of insulin activates phosphatidylinositol 3-kinase (PI3K) cascade, which is mainly involved in metabolic changes. Protein kinase B (Akt) is activated by PI3K mediated phosphorylation. Akt mediates a variety of key reactions from the insulin pathway, for example transfer of insulin sensitive glucose transporter 4 in the plasma membrane (Siddle 2011). On the other hand binding of insulin activates mitogen activated protein kinases/extracellular signal-regulated kinases (MAPK/ERK) cascade, which is mainly involved in cell growth related gene expression. Activation of MAPK/ERK cascade influences a variety of transcription factors (Sutherland et al. 2013). One downstream target of ERK is phosphorylated 90 kDa ribosomal S6 kinase (p90 RSK). Activated p90 RSK influences mRNA translation and protein synthesis (Taha und Klip 1999). It has been shown, that defects in the MAPK/ERK cascade can be associated with decreased cellular insulin sensitivity (Zhang et al. 2011) and probably complex gene regulatory events (Muller-Wieland et al. 2001).

Insulin binds to insulin-like growth factor 1 (IGF) receptor as well. IGF-receptor, a receptor tyrosine kinase, has a similar structure as the insulin receptor. Both receptors share common pathways.

4.2 Insulin-like growth factor 1 and insulin-like growth factor 1 signaling

IGF is mainly produced in the liver and secreted as a result of stimulation by growth hormone. IGF displays a high sequence similarity to proinsulin (Rinderknecht und Humbel 1978). IGF mediates anabolic effects on the organism and is growth-promoting and proliferating on almost every cell in the body (Yakar 2002). IGF binding to its receptor activates autophosphorylation and phosphorylation of insulin receptor substrates; hence the PI3K cascade and MAPK/ERK pathway are activated. Binding of insulin to IGF receptor and IGF to insulin receptor is possible, but associated with a lower affinity and potency (Rassow et al. 2008).

IGF as well as insulin signaling display pleiotropic effects in the heart, which are required for normal cardiac metabolism and function. Both signaling pathways influence physiological and pathophysiological heart conditions (Riehle und Abel 2016).

4.3 Cardiac insulin and insulin-like growth factor 1 signaling

Altered cardiac insulin and IGF signaling seem to play an important role in the development of heart failure. A healthy heart mainly uses free fatty acids as substrate. During advanced heart failure a substrate switch from fatty acids towards glucose occurs (Stanley und Chandler 2002). Insulin resistance inhibits this substrate switch, which has been suggested as adaptive response in the development of heart failure (Stanley et al. 2005).

Insulin and IGF signaling activate PI3K. Acute activation of PI3K/Akt has cardioprotective effects in models of cardiac injury (Yao et al. 2014). It has been suggested, that cardioprotection is achieved by elevating glucose metabolism, an anti-apoptotic effect and controlling cardiomyocyte growth (Matsui und Rosenzweig 2005). Furthermore, insulin and IGF signaling activate MAPK/ERK pathway. ERK activation is involved in hypertrophic response as well as heart failure and seems to be cytoprotective (Zhang et al. 2003).

To investigate insulin and IGF signaling in the heart, mice with cardiac inducible double knockout (dKO) of insulin receptor and IGF receptor or insulin receptor substrates 1 and 2 have been generated. Both models display overlapping phenotypes with heart failure and increased mortality. dKO mice show sarcomeric disarray and downregulation of genes involved in cardiac structure. In conclusion, loss of insulin and IGF signaling led to rapid disruption of sarcomeric structure and provide a critical mechanism for the development of heart failure (Riehle et al. 2015, unpublished results).

4.4 Sarcomere structure and function

Sarcomeres form the smallest unit of cardiac and striated skeletal muscles and are fundamental for their contraction. Long chains of sarcomeres are found in cardiomyocytes. To form a functional syncytium, cardiomyocytes are connected by gap junctions, which enable chemical communication and transfer electrical excitation between cells (Forbes und Sperelakis 1985). Each sarcomere contains multiple different structural proteins, whose arrangement give muscles their striated appearance under the light microscope. Thin filaments consisting of actin and thick filaments consisting of myosin are the contractile parts of a sarcomere (Behrends et al. 2010).

Besides actin and myosin another central protein is the troponin complex. The troponin complex is an important regulator of cardiomyocyte contraction. Troponin T anchors the troponin complex to tropomyosin. Troponin I is the inhibitory region and maintains actin to

tropomyosin binding, preventing myosin to actin binding at low intracellular calcium concentration. Troponin C binds the switch region of troponin I in a calcium-dependent manner to activate contraction. The troponin complex releases the binding site from actin to myosin, when the cell is stimulated for contraction (Hwang und Sykes 2015).
Proteins regulating sarcomere and cytoskeleton assembly are required for cardiac excitation-contraction coupling as well. An example of such a protein is PDZ and LIM Domain 5 (Pdlim5). Pdlim5 tethers protein kinases to the Z-line in striated muscles (Dixon et al. 2015). Alterations in sarcomeric protein composition lead to sarcomeric dysfunction with reduced cardiac pump function, which is often observed in heart failure (Hamdani et al. 2008).

4.5 Working hypothesis of the current study

Figure 1 shows the working hypothesis to investigate the connection between insulin signaling and regulation of sarcomeric protein expression in cardiomyocytes. As described above, insulin binds to its receptor on the cardiomyocyte´s cell surface and activates insulin signaling. MAPK/ERK pathway is activated and phosphorylates p90RSK. p90RSK contributes to the transcriptional activation of serum response factor (SRF). Myocardin is a transcriptional coactivator of SRF, they form a stable complex and bind to promoters on the DNA. Skeletal muscle alpha actin (Acta1) and smooth muscle alpha actin (Acta2) were described as SRF target genes.

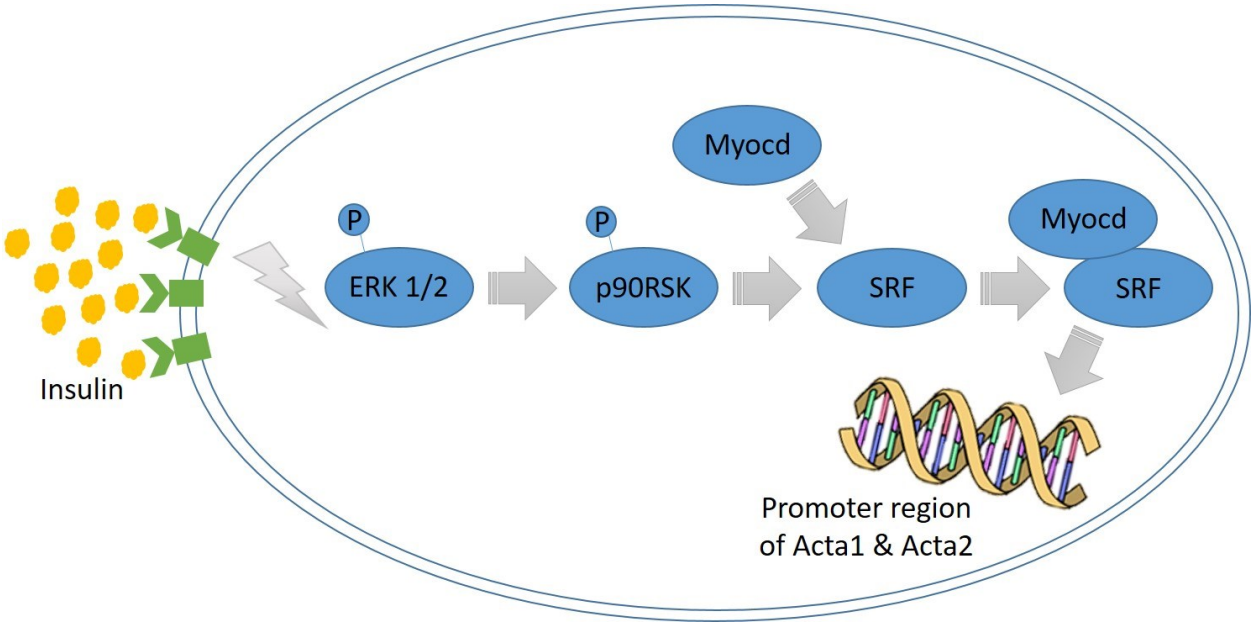

Figure 1. Working hypothesis of connection between insulin signaling and regulation of sarcomeric protein expression in cardiomyocytes, insulin (yellow dots) binds to insulin receptors (green rectangles) on cell surface. Flash indicates activation of insulin pathway. Arrows indicate activation. Phosphorylated (p), extracellular-signal-regulated kinases (ERK1/2), phosphorylated 90 kDa ribosomal S6 protein kinase (p90RSK), serum response factor (SRF), myocardin (Myocd), skeletal muscle alpha actin (Acta1), smooth muscle alpha actin (Acta2), diagram of double-stranded DNA source: Wikipedia

5 Aim of the study

Mice with cardiac inducible knockout of insulin receptor and insulin-like growth factor 1 receptor or insulin receptor substrate 1 and 2 have been generated previously. Both models displayed overlapping phenotypes with heart failure and increased mortality. Expression profiling revealed that several mRNAs coding for sarcomeric proteins were downregulated in these mice. These observations suggest a connection between insulin signaling and regulation of sarcomeric protein expression in cardiomyocytes.

How insulin signaling preserves contractile function by maintaining sarcomeric protein expression is incompletely understood. The aim of the current study was to take a closer look at insulin mediated regulation of sarcomeric protein expression through a serum response factor dependent mechanism.

6 Materials and methods

6.1 Materials

6.1.1 Buffers

Table 1. Buffer recipes

Buffer	Recipe
1x DNA extraction buffer	25 mM NaOH
	0.2 mM EDTA
20x TAE buffer	800 mM TRIS base
	400 mM acetic acid
	20 mM sodiumEDTA
1x RIPA buffer	50 mM TRIS-Cl pH 7.5
	150 mM NaCl
	0.2 mM Na_2EDTA pH 8.0
	0.2 EGTA pH 7.5
	1 % NP-40
	1 % sodium deoxycholate
	2.5 mM sodium pyrophosphate
20x MOPS buffer	1 M MOPS
	1 M TRIS base
	2% SDS
	0.02 M Na_2EDTA
10x transfer buffer	0.25 M TRIS
	1.92 M glycine
20x TBS	0.2 M TRIS base
	1.5 M NaCl
TBS/T	1xTBS
	0.1 % tween-20
	pH 7.6 with HCl

6.1.2 Primers

Table 2. Primer sequences

Use	Target	5'-3' sequence	
genotyping	Cre	forward	TGC CTG CAT TAC CGG TCG ATG
		reverse	CCA TGA GTG AAC GAA CCT GGT CG
	rtTA	forward	GTC GCT AAA GAA GAA AGG GAA ACA C
		reverse	TTC CAA GGG CAT CGG TAA ACA TCT G
qPCR	Acta1	forward	CCT GTA TGC CAA CAA CGT CA
		reverse	CTC GTC GTA CTC CTG CTT GG
	Acta2	forward	GTC CCA GAC ATC AGG GAG TAA
		reverse	TCG GAT ACT TCA GCG TCA GGA
	Cops6	forward	TGA CTG GGA GTG TTT CCG TC
		reverse	GAG CCC CAA TCA CCT GCA TAG
	Gja1	forward	ACA GCG GTT GAG TCA GCT TG
		reverse	GAG AGA TGG GGA AGG ACT TGT
	Myh7	forward	AGG AGC AAC AGG AGG ACT TCA
		reverse	CTC TGC ATT GGT GGG ATT GGT
	ANP	forward	GAG TGG ACT AGG CTG CAA CA
		reverse	CAC ACC ACA AGG GCT TAG GA
	BNP	forward	TTT GGG CTG TAA CGC ACT GAA
		reverse	AAA GAG ACC CAG GCA GAG TCA
	Pdlim5	forward	TGA GAC AGA CTA CTA CGC CC
		reverse	TCC CAG AGC TTC CAG ATA CA
	Tnni2	forward	TTC GGA GGG TGC GTA TGT CT
		reverse	GTC CCG TTC CTT CTC AGT GT
	Tnnt1	forward	AAC AAT GCC TGT GGT TCT TCC
		reverse	TGT GCT CTA CAA CCG CAT CA
	Trim63	forward	GTG TGA GGT GCC TAC TTG CTC
		reverse	GCT CAG TCT TCT GTC CTT GGA

cloning	Myocardin	gccactgtgctggatgccaccATGACACTCCTGGGGTCTG
		ggtggaattctgcagatTTACCACTGCTGTAAGTGGAG
	SRF	gccactgtgctggatgccaccATGTTACCGAGCCAAGCTG
		ggtggaattctgcagatTCATTCACTCTTGGTGCTG
	Acta1	tacgcgtgctagcccCCTCTAGGTCCCAACAGTTC
		gcagatctcgagcccCAGGTTTTTATATAGTCCCGG
	Acta2	tacgcgtgctagcccCTCTTTTCTTGTCTTTTAAAGGAATTG
		gcagatctcgagcccCTTGCTCTGATCCCCTCC

Cloning primers include lowercase backbone-specific sequence and uppercase insert-specific sequence.

6.1.3 Kits

Table 3. Kits

Kit	**Company**
Direct-zol™ RNA MiniPrep	Zymo Research
High-Capacity cDNA Reverse Transcription Kit	Applied Biosystems
Pierce BCA Protein Assay Kit	Thermo Fisher Scientific
Pierce Primary Cardiomyocyte Isolation Kit	Thermo Fisher Scientific
PureLink Quick Plasmid Miniprep Kit	Invitrogen
Plasmid Maxi Kit	Qiagen
Dual-Luciferase® Reporter Assay System	Promega

6.1.4 Antibodies

Table 4. Primary and secondary antibodies

Primary	GAPDH (14C10)	Cell Signaling, Rabbit #2118
	α-tubulin	Sigma, T5168, Mouse
	phospho-Akt (Ser473)	Cell Signaling, Rabbit #9271
	Akt (pan) (40D4)	Cell Signaling, Mouse #2920
	phospho-p44/42 MAPK (Thr202/Tyr204)	Cell Signaling, Rabbit #9101
	p44/42 MAPK (Erk1/2) (3A7)	Cell Signaling, Mouse #9107
	phospho-p90RSK (Ser380) (D5D8)	Cell Signaling, Rabbit #12032
	RSK1/RSK2/RSK3 (32D7)	Cell Signaling, Rabbit #9355

	SRF (D71A9) XP	Cell Signaling, Rabbit #5147
	Myocardin	R&D Systems, 4028, Mouse #355521
	insulin receptor β (L55B10)	Cell Signaling, Mouse mAb #3020
	IGF-I receptor β (111A9)	Cell Signaling, Rabbit #3018
Secondary	goat anti-rabbit IgG	Thermo Fisher, Alexa Fluor® 680
	goat anti-mouse IgG	Thermo Fisher, Alexa Fluor® 680

6.1.5 Cell culture

Chinese hamster ovary cells overexpress human insulin receptor and were a kind gift of Morris F. White, Harvard Medical School Boston (Backer et al. 1992).

Table 5. Cell culture media

Media	**Company**
DMEM/F12	Gibco
Penicillin-Streptomycin (10,000 Units/ml)	Gibco
Trypsin-EDTA (0.05%), phenol red	Gibco
Fetal Bovine Serum - Premium	Atlanta Biologicals
DMEM, low glucose	Gibco

6.1.6 Plasmids

pcDNA3.1 plasmid was derived from Invitrogen and confers ampicillin resistance for selection in bacteria. The reporter plasmid pGL3_basic was derived from Promega and confers an ampicillin resistance as well. Promoters of Acta1 and Acta2 were cloned into the SmaI digestion site upstream of the firefly luciferase coding sequence. pRL-SV40 and CMV vectors were derived from Promega and encoded renilla luciferase.

6.2 Methods

6.2.1 Housing conditions and mouse colony

Transgenic mice and Wistar rats were housed on a 12 hour light/12 hour dark cycle at 22°C with free access to food (2020X Teklad Global Soy Protein-Free Extruded Rodent Diet) and water. All experiments were performed in accordance with protocols approved by the Carver College of Medicine of the University of Iowa.

The doxycycline inducible cardiac specific insulin-like growth factor 1 receptor and insulin receptor deficient mice (cIR-IGFRdKO) were generated by developing compound transgenic mice harboring a tet-on Cre (purchased from Jackson lab, strain number 6234), an rtTA under the control of the αMHC promoter and two floxed IGF receptor as well as insulin receptor alleles. All mice were back-crossed to the C57/BL6 genetic background.

For the induction 8-week-old cIR-IGFRdKO mice were intraperitoneal injected with doxycycline (doxycycline hyclate, sigma) 4mg/kg body weight and kept on doxycycline chow (1g/kg) for 1 week. At the age of 9 week the mice were sacked. After anesthesia 0.01 U/g body weight of insulin or saline was injected into the inferior vena cava. After 10 minutes the tissues were collected and immediately frozen in liquid nitrogen until further use. The right tibia was collected as well, freed from tissue in 1 M NaOH at 90°C for 20 minutes and the length measured.

6.2.2 Genotyping of mice

To obtain DNA from each mice an ear punch was taken, digested in 80 µl DNA extraction buffer at 98°C for 1 hour and afterwards 80 µl of 40 mM TRISHCl pH 5.5 were added.

- 9.5 µl water
- 10 µl 2x ChoiceTaq master mix
- 0.5 µl primer mix
- 2 µl DNA

Mix was prepared and ran with the protocol from table 6. The resulted product was separated on 2% agarose gel in 1x TAE buffer with ethidium bromide for about 20-30 minutes under a voltage of 120 volt. A picture was taken with the VWR Gel Imager.

Table 6. PCR protocol

Function		Temperature	Time
initial denaturation		94°C	3 min
	denaturation	94°C	45 sec
40 cycles	annealing	54°C for Cre, 62°C for rtTA	30 sec
	extension	72°C	30 sec
final hold		72°C	2 min
cool down		4°C	until use

6.2.3 Quantitative polymerase chain reaction

Sample preparation

NRCM were directly lysed with a cell scraper in TRIzol (life technologies). Heart tissue pieces were homogenized in the TissueLyserII (Qiagen) in TRIzol. The purification of mRNA was performed with the Direct-zol™ RNA MiniPrep from Zymo Research based on the company's protocol, which includes a DNAse I treatment.

The purity control and concentration measurements of mRNA samples were performed with the NanoDrop2000. 2 µl of each sample were analyzed. The ratios of absorbance at 260/280 as well as 260/230 were used to assess the purity of mRNA and DNA.

The mRNA was transcribed in cDNA with the High-Capacity cDNA Reverse Transcription Kit. mRNA was mixed with 2x Reverse Transcription master mix from the kit and run in a thermocycler based on the company's protocol. Afterwards, a standard curve was generated and nuclease-free water added to each sample.

Primer design and melting curve

Primer Blast (http://www.ncbi.nlm.nih.gov/tools/primer-blast/) was used to design the quantitative polymerase chain reaction (qPCR) primers with the following inclusions: amplicon length approximately 75–150 base pairs, primer 18–24 nucleotides in length and free of internal secondary structure, primer pairs with compatible melting temperatures and approximately 50% guanine-cytosine content. To allow differentiation between amplification of the desired cDNA and potential contaminating genomic DNA an exon/intron selection was preferred. The designed primers were ordered at Integrated DNA Technologies (IDT

Coralville). To test the primer's specificity for cDNA a regular PCR with cDNA and genomic DNA for each primer was performed.

A melting curve was produced at the end of 40 qPCR cycles. The temperature was raised slowly and fluorescence continuously measured. Primers with one melting curve peak were used.

qPCR and Quantification

Samples were pipetted in triplicate in a 384 well plate:

- 4.5 µl diluted cDNA
- 0.25 µl 4 µM forward primer
- 0.25 µl 4 µM backward primer
- 5 µl Power SYBR® Green master mix

Table 7. qPCR protocol

Function		Temperature	Time
initial denaturation		95°C	10 min
40 cycles	denaturation	95°C	15 sec
	annealing	60°C	1 min
	extension	72°C	1 min
melting curve		60° - 95°C	0.05°C increase every sec
cool down		4°C	until use

The measuring instrument (QuantStudio™ 7 Flex Real-Time PCR System) generated an amplification plot by plotting fluorescence signal against the cycle numbers.

QuantStudio™ Software V1.2 for QuantStudio™ 6 and 7 Flex was used. The software automatically set a threshold. Threshold cycle reflected the cycle number at which the fluorescence generated within a reaction crossed the threshold. The software averaged triplicate of each sample and calculated under use of the standard curve quantity means. For normalization of expression levels between experiments COP9 signalosome complex subunit 6 (Cops6) was used as a housekeeping gene.

6.2.4 Western blot

Sample preparation and BCA

NRCM were directly lysed in RIPA buffer with Halt™ Protease and Phosphatase Inhibitor Cocktail. Heart tissue pieces were homogenized in the TissueLyserII (Qiagen) in RIPA buffer with Halt™ Protease and Phosphatase Inhibitor Cocktail. The total protein concentration was determined with the Thermo Scientific Pierce BCA Protein Assay Kit. A standard curve of bovine serum albumin and the samples were pipetted in triplicate into a 96 well plate and measured by the Epoch Microplate Spectrophotometer. The results were analyzed with the Gen5 Data Analysis software. Based on the concentration, the amount of protein necessary was calculated and mixed with NuPAGE® LDS sample buffer (4x), 2-mercaptoethanol (2.5%) and filled up to 20 µl with RIPA-Buffer. The samples were heated to 70°C for 10 minutes for denaturation.

Western Blot

The sample and a molecular weight marker (Odyssey® Protein Molecular Weight Marker (10-250 kDa)) were loaded in the wells of a NuPAGE™ Novex™ 4-12% Bis-Tris Gel. The gel was run in 1x MOPS buffer with NuPAGE® Antioxidant for 1 hour at 200 volt to separate the samples based on their size. Proteins were moved from the gel to a polyvinylidene fluoride membrane (IPFL00010, Immobilon-FL) by electric field. Transfer conditions were 0.2 ampere for 2 hours in 1x transfer buffer with 20% methanol at 4°C.

Membranes were blocked for 1 hour in 5% bovine serum albumin TBS/T, incubated overnight in primary antibody (dilution 1:1000), washed three times 5 minutes each with TBS/T, incubated for 1 hour with secondary antibody (dilution 1:20000) and washed again.

For detection of the fluorescent secondary antibody the Odyssey CLx Infrared Imaging System from LI-COR was used. The image was analyzed with the Image Studio Lite software. Protein contents were normalized by Glyceraldehyde-3-phosphate dehydrogenase (GAPDH) or α-tubulin.

6.2.5 Cell culture

Neonatal rat cardiomyocytes

Neonatal rat cardiomyocytes (NRCM) were isolated on day 3 of Wistar rat pups with the Thermo Scientific Pierce Primary Cardiomyocyte Isolation. The dishes for cultivation were coated with collagen type 1 rat tail. Two neonatal rat hearts were pooled in one tube and isolated based on the kit's protocol. NRCM were kept in an incubator with 5% CO and 37°C humidified air. As recommended 10 % heat inactivated fetal bovine serum and 1 % penicillin-streptomycin were added to media. 24 hours after isolation media were changed and growth supplement was added. On day 4 or 5 after isolation the NRCM were starved in serum free, low glucose DMEM media and treated on the next day.

CHO-IR cells and transfection

Chinese hamster ovary cells overexpress human insulin receptor (CHO-IR) were cultured in DMEM/F-12 media with 10 % fetal bovine serum and 1 % penicillin-streptomycin on 10 cm dishes in an incubator with 5% CO and 37°C humidified air. For cell culture passing Trypsin/EDTA 0.05% solution was used. The splitting was done every 2-3 days with a 1:10 dilution.

For transfection 100000 CHO-IR cells (Z Series Coulter Counter) were plated in each well from a 6 well dish in serum free DMEM/F-12 media. Cells were transfected with Lipofectamine 2000 in a ratio of 1:3. 350 ng SRF or an empty pcDNA3.1 plasmid, 350 ng myocardin or an empty pcDNA3.1 plasmid and 350 ng Acta1 or Acta2 or an empty pGL3_basic plasmid and 0.35 ng of SV40 or CMV renilla plasmid were mixed for each well. A total amount of 100 µl serum free media with about 1 µg of DNA and 3 µl of Lipofectamine was transfected into each well.

6.2.6 Cloning

Gibson assembly

pcDNA3.1 was digested with EcoRV and pGL3_basic with SmaI. SRF was amplified from mouse heart cDNA and myocardin from the Addgene Plasmid #46033. The promoter regions of Acta1 and Acta2 were amplified from genomic mouse DNA.

These reactions were performed with the Q5 High-Fidelity 2x master mix:

- 12.5 µl Q5 High-Fidelity 2x master mix
- 2.5 µl 10 µM forward and reverse primer (designed by NEBbuilder assembly tool)
- 1 µl template DNA (100 ng of cDNA or genomic DNA)
- 9 µl nuclease-free water

Table 8. High-Fidelity PCR protocol

Function		Temperature	Time
initial denaturation		98°C	30 sec
30 cycles	denaturation	98°C	10 sec
	annealing	myocardin and SRF 63.5°C, Acta1 and Acta2 61°C	20-30 sec/kb
	extension	72°C	1 min
final extension		72°C	2 min
cool down		4°C	until use

HiFi DNA assembly protocol from NEBbuilder assembly tool was used for Gibson assembly. Gibson assembly reaction was set up with 10 µl of 2x assembly master mix, the calculated amount of insert and backbone and filled up with water to 20 µl. This mix was incubated at 50°C for 30 minutes.

Transformation of competent cells

NEB 5alpha competent E. coli cells were transformed with 2 µl of the assembled product, placed for 30 minutes on ice, heat shocked for 30 seconds at 42°C and placed back on ice for 2 minutes. 950 µl SOC medium at room temperature was added to each tube and incubated for 1 hour at 37°C while shaking.

20 grams lysogeny broth were stirred into 1 liter of water and 15 grams of bacto agar were added. This solution was autoclaved and cooled down to 55°C to add 100 µg/ml ampicillin, used for selection of transfected cells. 20 ml were poured into 100x15 mm petri dishes, they were stored at 4°C until use. Prior to use a lysogeny broth agar plate was warmed up to 37°C. 100 µl of the transformed cells were spread on the plate and incubated overnight at 37°C.

Analysis of insert

Amplification of the cloned fragment was screened by PCR, plasmids from that colony were purified with the Quick Plasmid Miniprep Kit (Invitrogen). 200 ng purified plasmids were digested with restriction enzyme. Acta1 in pGL3-basic and myocardin in pcDNA3.1 were digested with BglIII, Acta2 in pGL3_basic with AseI and SRF in pcDNA3.1 with BlpI. After one hour digestion a distinct fragment pattern was shown on 1% agarose gel.

Plasmid were Sanger sequenced at the Iowa Institute of Human Genetics with the Applied Biosystems Model 3730 (48-capillary) and Model 3730xl (96-capillary) DNA Sequencers. The resulted fluorescent peak trace showed the correct order of nucleotides.

DNA from the colony with confirmed insert was isolated by using the Qiagen Maxi Kit.

6.2.7 Luciferase Assay

As described in the cell culture section, CHO-IR cells were transfected with two different types of luciferase vectors. The resulting transcription products were firefly and renilla luciferase, which were able to convert luciferin into oxyluciferin under light emission. The Dual-Luciferase Assay System was used from Promega and measurements were carried out in the GloMAx Promega luminometer. The transfected CHO-IR cells were lysed in 100 µl of passive lysis buffer. 10 µl of this lysate was pipetted in triplicates to the 96well plate for luciferase activity measurement. First 50 µl of luciferase assay reagent was added to each well and the firefly light emission monitored for 5 seconds. After a 5 seconds delay, 50 µl of stop & glow reagent was added and the renilla light emission monitored for 5 seconds. Firefly luciferase activity was normalized to renilla luciferase acticity, which was used as control of transfection efficiency into CHO-IR cells.

6.2.8 Statistical analysis

The mean, standard deviation and t-test were calculated with Microsoft Excel and expressed as mean values ± standard deviation with n denoting the number of experiments. GraphPad Prism 5 was used for the creation of graphics. Data are expressed as fold change or relative expression to control values. Differences were considered statistically significant at a p value of <0.05, this is indicated by an asterisk.

7 Results

7.1 Characteristics of dKO mice (Riehle et al. 2015)

Riehle et al. used cardiac inducible double knockout mice of insulin receptor and insulin-like growth factor 1 receptor (cIR-IGFRdKO) or insulin receptor substrate 1 and 2 (cIRSdKO) to study the effects of a loss of insulin signaling in the adult hearts. Both models displayed cardiac dysfunction and sarcomeric disarray as early as one week after knockout induction. Expression profiling revealed that several mRNAs coding for sarcomeric proteins were downregulated in dKO mice, decreased mRNA levels of genes involved in cardiac structure as early as three days (fast skeletal muscle troponin I, slow skeletal muscle troponin T, gap junction protein (Gja1), myosin light chain 1, skeletal muscle alpha actin (Acta1), and smooth-muscle alpha actin (Acta2) by 52-82%, $p<0.05$ each). Accordingly, electron micrographs revealed loss of sarcomeric integrity as early as 3 days post-deletion of insulin receptor and insulin-like growth factor 1 (IGF) receptor or insulin receptor substrates 1 and 2. In general the sarcomeric structure was less organized. The M- and Z-lines were diffused degraded and less intense. The intercalated disks were pulling apart.

7.2 cIR-IGFRdKO mice displayed reduced heart weight

Table 9 lists the male and table 10 the female body, lung and heart weights and tibia length of 9-week-old wildtype (WT) and cIR-IGFdKO (KO) mice, one week after knockout induction. Body and lung weights were not different between WT and KO, neither the lung to body weight ratios, in both sexes. KO hearts weighed 15% less than WT hearts in both sexes. Female mice presented with lower body weight and lower heart weight compared to males. Nevertheless, heart to body weight ratios from both sexes were similar for the same genotype.

Table 9. Body weight (BW), lung weight (LW), heart weight (HW) and tibia length of 9-week-old male cardiac inducible double knockout of insulin receptor and insulin-like growth factor 1 receptor (KO) and wildtype mice (WT), one week after knockout induction.

variable	WT	KO	p value
BW (g)	22.8 ± 1.8	23.0 ± 2.6	0.8802
LW (mg)	146.8 ± 6.4	151.8 ± 13.8	0.3335
HW (mg)	106.7 ± 7.1	91.3 ± 8.8	0.0007
Tibia length (mm)	16.5 ± 0.4	16.4 ± 0.4	0.6547
BW/Tibia length	1.39 ± 0.09	1.40 ± 0.13	0.7638
LW/BW	6.45 ± 0.27	6.63 ± 0.39	0.2682
HW/BW	4.68 ± 0.20	3.98 ± 0.21	0.0000

Mean ± standard deviation of mean, n=10

Table 10. Body weight (BW), lung weight (LW), heart weight (HW) and tibia length of 9-week-old female cardiac inducible double knockout of insulin receptor and insulin-like growth factor 1 receptor (KO) and wildtype mice (WT), one week after knockout induction.

variable	WT	KO	p value
BW (g)	16.3 ± 1.6	17.3 ± 1.6	0.3761
LW (mg)	123.2 ± 12.8	125.8 ± 9.5	0.7232
HW (mg)	81.8 ± 8.2	70.2 ± 5.8	0.0286
Tibia length (mm)	15.6 ± 0.4	15.7 ± 0.3	0.6839
BW/Tibia length	1.05 ± 0.10	1.10 ± 0.09	0.3807
LW/BW	7.55 ± 0.29	7.32 ± 0.54	0.4286
HW/BW	5.02 ± 0.26	4.08 ± 0.22	0.0001

Mean ± standard deviation of mean, n=6

7.3 Cardiac insulin receptor and IGF receptor protein expression was reduced one week after knockout induction in cIR-IGFRdKO mice

Figure 2 shows cardiac insulin receptor and IGF receptor protein expression in 9-week-old mice one week after knockout induction. The insulin receptor and IGF receptor levels were decreased in KO compared to WT in both sexes.

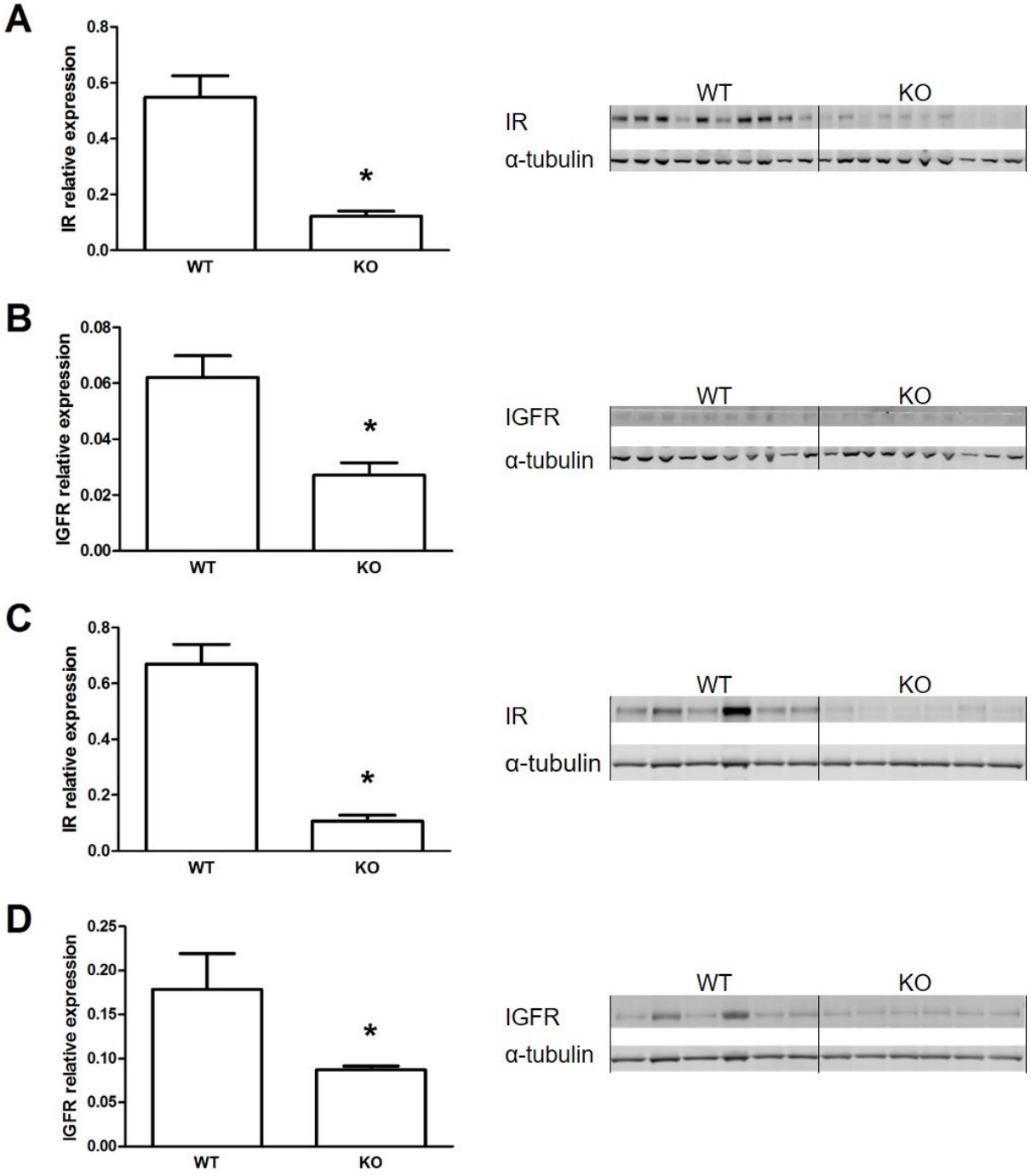

Figure 2. Cardiac protein expression in 9-week-old cardiac inducible double knockout of insulin receptor and insulin-like growth factor 1 receptor (KO) and wildtype mice (WT), one week after knockout induction, (A) level of insulin receptor (IR) in male KO and WT, (B) level of insulin-like growth factor receptor (IGFR) in male KO and WT, (C) level of IR in female KO and WT, (D) level of IGFR in female KO and WT, values were normalized to α-tubulin and presented as mean ± standard deviation of mean. *$p < .05$ compared to WT, n=10 for male, n=6 for female

7.4 Reduced Acta1 mRNA expression in female cIR-IGFRdKO mice

Figure 3 shows mRNA expression levels of sarcomeric proteins and heart failure markers in 9-week-old female cIR-IGFRdKO mice one week after knockout induction. A significant increase was seen in the mRNA expression levels of atrial natriuretic peptide (ANP) and brain natriuretic peptide (BNP). mRNA expression of sarcomeric proteins showed a significant reduction in Acta1. Acta2 (p=0.23), Gja1 (p=0.06), PDZ and LIM domain 5 (Pdlim5) (p=0.24) and cardiac muscle troponin T (Tnnt2) (p=0.15) expression levels remained unchanged. Cardiac beta myosin heavy chain (Myh7) and slow skeletal muscle troponin I (Tnni1) presented with high variability.

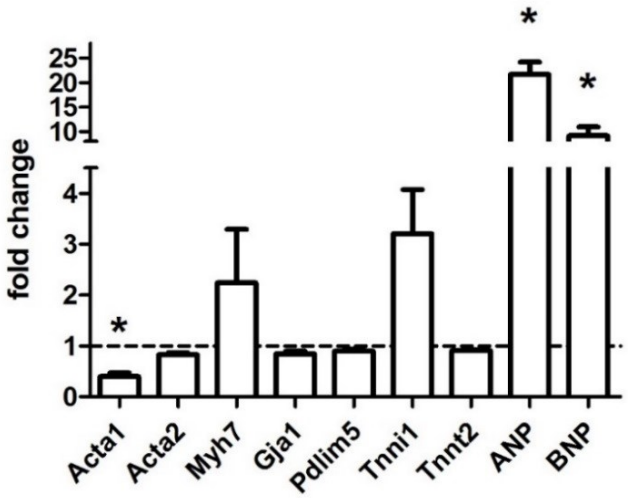

Figure 3. mRNA expression levels of sarcomeric related genes and heart failure markers in 9-week-old female cardiac inducible double knockout of insulin receptor and insulin-like growth factor 1 receptor one week after knockout induction, skeletal muscle alpha actin (Acta1), smooth muscle alpha actin (Acta2), cardiac beta myosin heavy chain (Myh7), gap junction protein (Gja1), PDZ and LIM domain (Pdlim5), slow skeletal muscle troponin I (Tnni1), cardiac muscle troponin T (Tnnt2), atrial natriuretic peptide (ANP) and brain natriuretic peptide (BNP), values were normalized to Cops6 and presented as mean ± standard deviation of mean. *p < .05 compared to wildtype, n=4

7.5 Insulin stimulation led to increased Acta1 and Acta2 expression in NRCM

Figure 4 shows mRNA expression levels from sarcomeric related genes (Acta1, Acta2, Myh7, Gja1, Pdlim5, Tnni1, Tnnt2) in NRCM after insulin stimulation. Insulin stimulation was checked for efficiency assessing tripartite motif containing 63 (Trim63) downregulation ($p<0.05$ for 4 and 24 hours, $p=0.12$ for 48 hours). Overall both actin genes showed the biggest increase: Acta1 was significantly upregulated in all stimulated NRCM and Acta2 after 24 and 48 hours of stimulation.

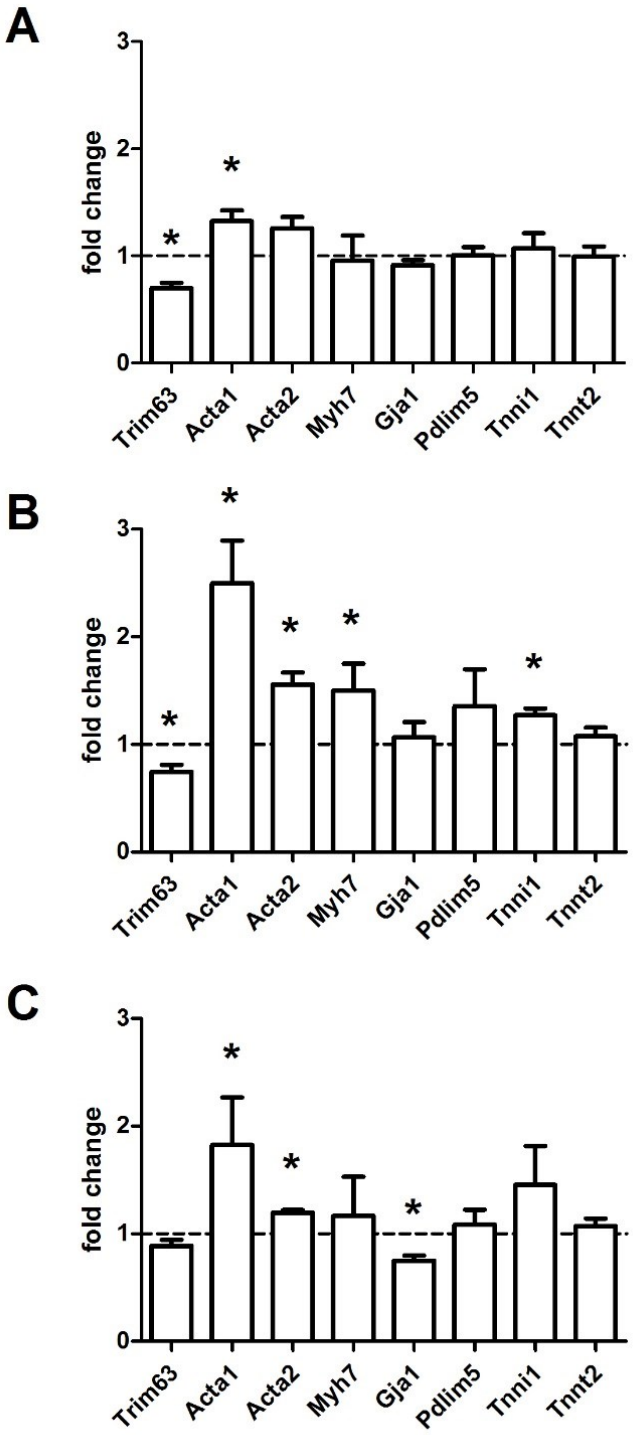

Figure 4. mRNA expression levels of sarcomeric related genes in NRCM after (A) 4 hours, (B) 24 hours and (C) 48 hours of 500 nM insulin stimulation, tripartite motif containing 63 (Trim63) as insulin stimulation control, skeletal muscle alpha actin (Acta1), smooth muscle alpha actin (Acta2), myosin heavy chain (Myh7), gap junction protein (Gja1), PDZ and LIM domain (Pdlim5), troponin I (Tnni1), troponin T (Tnnt2), values were normalized to Cops6 and presented as mean ± standard deviation of mean. *$p < .05$ compared to unstimulated control, n=3 for (A) and (C), n=5 for (B)

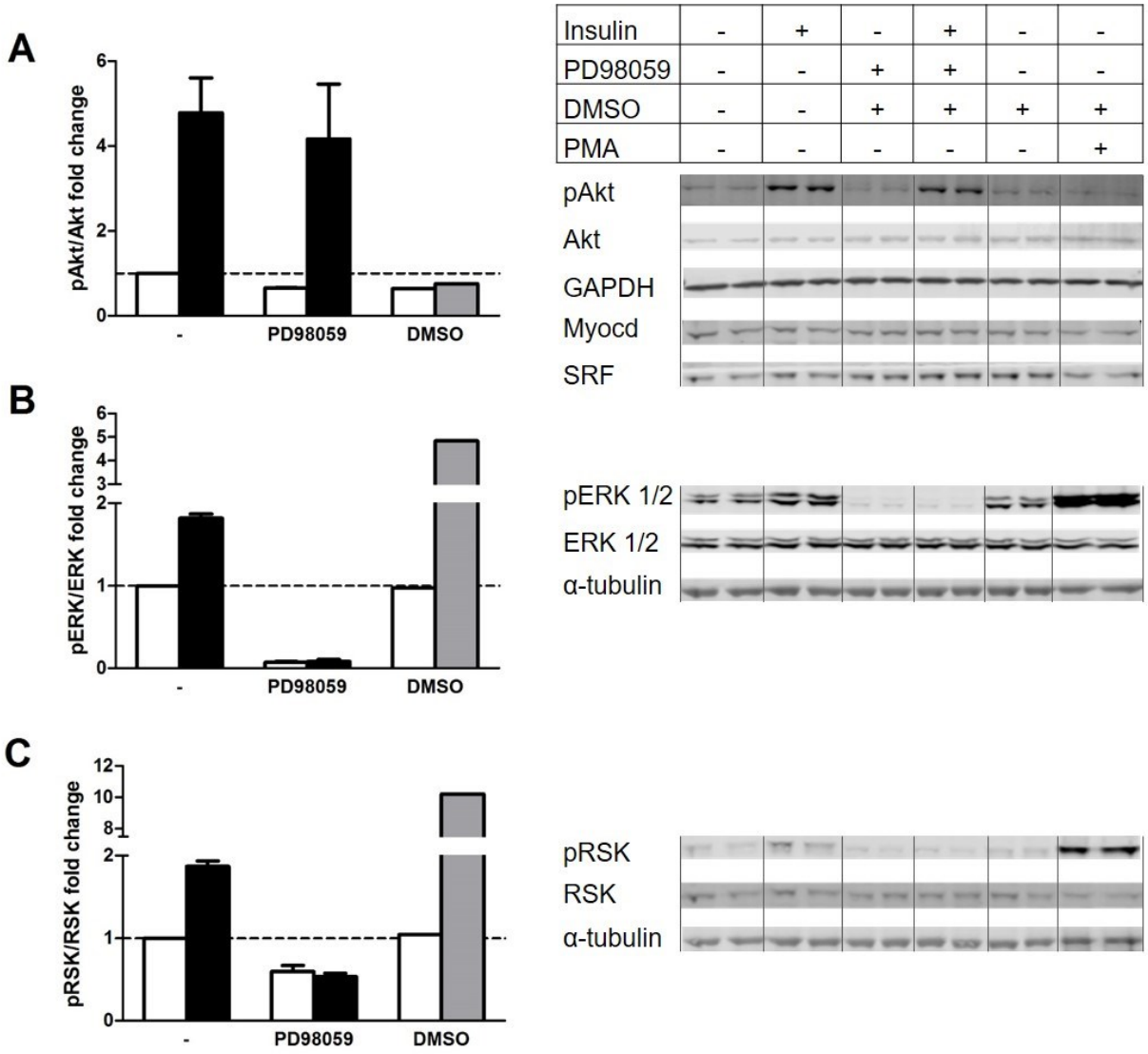

Figure 5. Protein expression in 100 nM insulin or 1 µM phorbol 12-myristate 13-acetate (PMA) stimulated NRCM, open bars indicate control, black bars insulin and grey bars PMA stimulated, dimethylsulfoxide (DMSO) was vehicle for 10 µM ERK inhibition (PD98059) and PMA treatment (A) level of phophorylated Akt at Ser473 to total Akt protein, myocardin (Myocd) and serum response factor (SRF) checked for presense and not quantified (B) level of phosphorylated ERK 1/2 at Thr202/Tyr204 to total ERK protein, (C) level of phosphorylated p90RSK at Ser380 to total RSK protein, values were normalized to GAPDH or α-tubulin and presented as mean ± standard deviation of mean for no (-) and PD98059 treatment or presented as mean for DMSO. n=4 for - and PD98059 treatment, n=2 for DMSO

7.6 ERK inhibition prevented ERK and RSK phosphorylation, and may inhibit insulin induced Acta1 and Acta2 expression

Figure 5 shows phosphorylated to total protein expressions in insulin or phorbol 12-myristate 13-acetate (PMA) stimulated NRCM with or without ERK inhibition. Presence of myocardin and serum response factor (SRF) in NRCM was shown. PMA stimulation led to an increased level of phosphorylated ERK 1/2 at Thr202/Tyr204 to total ERK protein and an increased level of phosphorylated p90RSK at Ser380 to total RSK protein. PMA is an activator of protein kinase C and was more efficient in ERK and RSK activation than insulin stimulation. Insulin stimulation led to an increased level of phophorylated Akt at Ser473 to total Akt protein, an increased level of phosphorylated ERK 1/2 at Thr202/Tyr204 to total ERK protein and an increased level of phosphorylated p90RSK at Ser380 to total RSK protein. ERK inhibition in NRCM completely abolished insulin-induced ERK and RSK activation. Insulin-induced Akt activation was unaffected by ERK inhibition.

Figure 6 shows mRNA expression levels of Acta1 and Acta2 in insulin stimulated NRCM with or without ERK inhibition. Insulin stimulation led to an increase in Acta1 and Acta2 mRNA expression. However, the increase was blunted with ERK inhibition. The results are difficult to interpret give the strong decrease in basal mRNA expression of Acta1 and Acta2 with ERK inhibition. Acta1 expression within one replicate was equal with or without ERK inhibition. Acta2 expression within one replicate was higher without ERK inhibition. This indicates a high degree of variability in the experiments which requires additional replicates to definitively determine the role of ERK in insulin activated Acta1 and Acta2 expression.

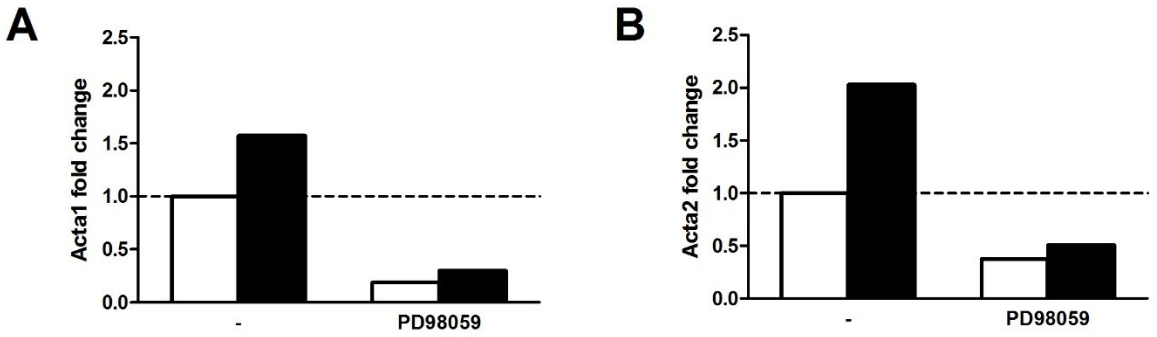

Figure 6. mRNA expression of (A) skeletal muscle alpha actin (Acta1) and (B) smooth muscle alpha actin (Acta2) in NRCM after 24 hours of 500 nM insulin stimulation with or without 10 μM ERK inhibition (PD98059), open bars indicate control, solid bars insulin stimulated, values were normalized to Cops6 and presented as mean, n=2

7.7 Insulin stimulation led to ERK and RSK phosphorylation in CHO-IR cells

Figure 7 shows phosphorylated to total protein expressions in insulin-stimulated Chinese hamster ovary cells overexpress human insulin receptor (CHO-IR). Insulin stimulation led to increased level of phosphorylated ERK 1/2 at Thr202/Tyr204 to total ERK protein and an increased level of phosphorylated p90RSK at Ser380 to total RSK protein. Higher insulin concentration did not lead to further increase of ERK and RSK activation. Maximal activation was already achieved with 100 nM. Furthermore, the maximal extent of phosphorylation was before 30 minutes, because the earlier time point of 15 minutes showed a higher ERK and RSK activation than the later one.

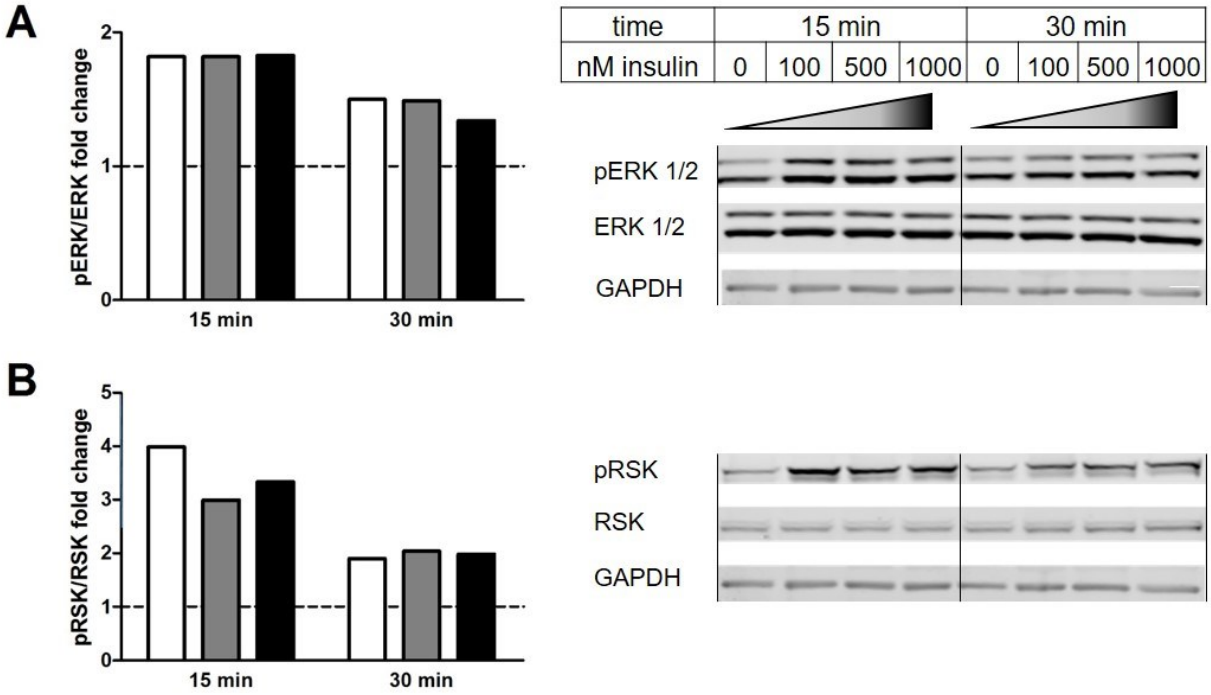

Figure 7. Protein expression in insulin stimulated CHO-IR cells after 15 and 30 minutes, open bars indicate 100 nM insulin, grey bars 500 nM insulin, black bars 1000 nM insulin, (A) level of phosphorylated ERK 1/2 at Thr202/Tyr204 to total ERK protein, (B) level of phosphorylated p90RSK at Ser380 to total RSK protein, values were normalized to GAPDH, n=1

7.8 Acta1 and Acta2 promoter activities were not stimulated by insulin

Figure 8 shows Acta1 and Acta2 promoter activities 24 hours after transfection into CHO-IR cells. PMA treatment served as positive control for the setup, inducing SRF activity and leading to elevated promoter activities. Transfection without myocardin led to reduced promoter activities compared to baseline and served as negative control, because SRF can only bind to DNA with its coactivator myocardin. Acta1 promoter insert showed in all treatments about 25 times higher activity than pGL3_baisc. Acta2 promoter insert showed in all treatments about 5 times higher activity than pGL3_basic. Acta1 and Acta2 promoter activities did not show a specific effect in response to insulin. Insulin stimulated Acta1 promoter activity and Acta2 promoter activity in a similar strength as a luciferase plasmid with minimal promoter (pGL3_basic).

Figure 9 shows Acta1 and Acta2 promoter activities 24 hours after transfection into CHO-IR cells. This measurement, normalized to CMV renilla luciferase, obtained similar results to the promoter activities from Figure 8, where firefly activity was normalized to SV40 renilla luciferase. Transfection without myocardin led to reduced promoter activities compared to baseline. Insulin or IGF stimulation had no effect on promoter activities in cells lacking myocardin. Activities were similar to untreated cells without myocardin. Insulin as well as IGF stimulation of transfected cells led to increased promoter activities. Acta1 promoter activity was about 25 times and Acta2 promoter activity about 4 times higher than pGL3_basic activity. Acta1 and Acta2 promoter activities did not show a specific effect in response to insulin and IGF. Insulin as well as IGF stimulated Acta1 promoter activity and Acta2 promoter activity in a similar strength as a luciferase plasmid with minimal promoter (pGL3_basic). While there seems to be a general activation in promoter activity, this may not be promoter activity at all. Because the pathways being activated regulate protein synthesis, the luciferase activity could be simply an increase in protein synthesis. Therefore, the increase in pGL3 basic could be due to increased protein synthesis and not SRF/Myocardin activity. However, Figure 9B suggests that myocardin is necessary for the induction in pGL3 basic activity. Again, interpretation of these results is difficult given the small sample size. This requires further replication to determine if Acta1 and Acta2 promoter activities induced by insulin or IGF are generic or dependent on SRF.

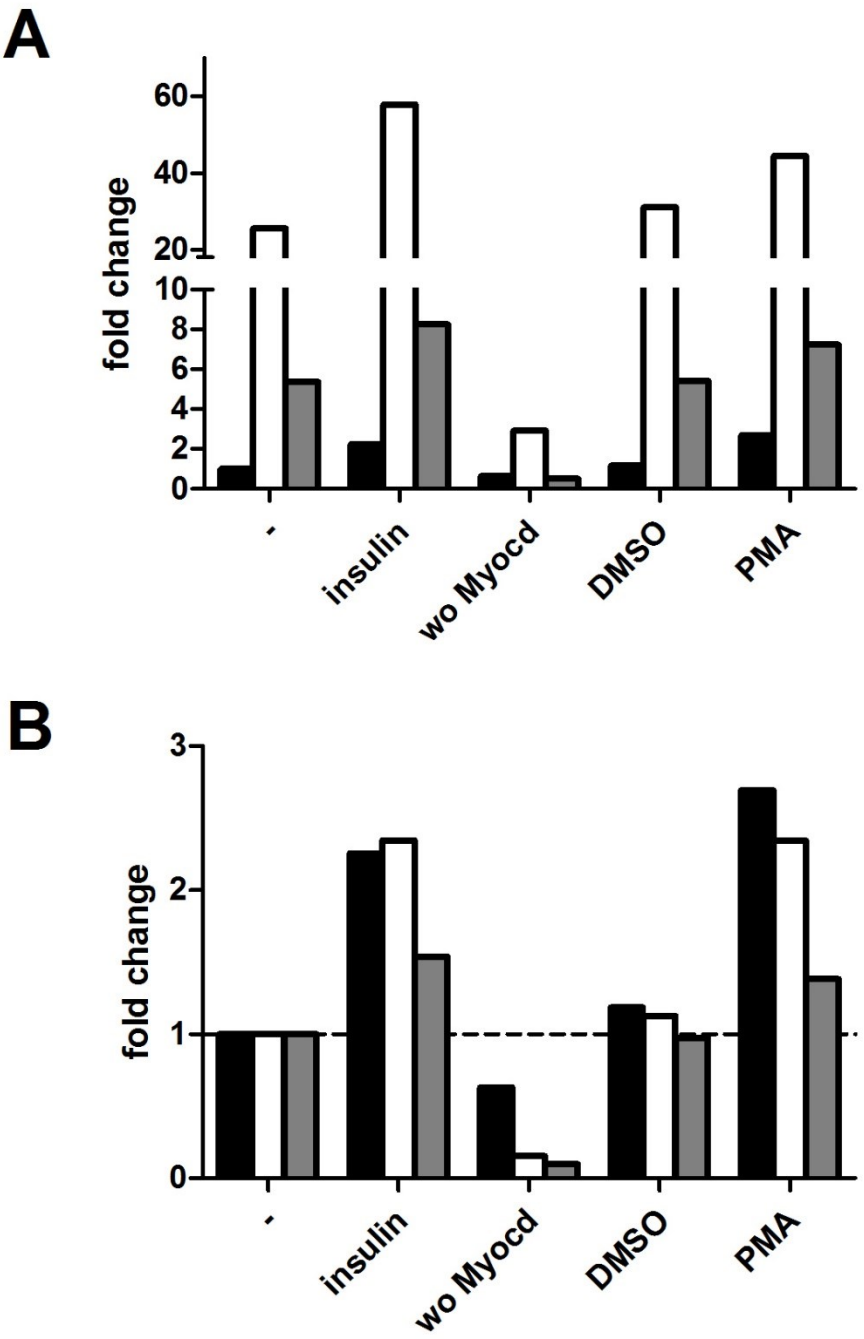

Figure 8. Empty pGL3_basic, skeletal muscle alpha actin (Acta1) and smooth muscle alpha actin (Acta2) promoter activities 24 hours after transfection into CHO-IR cells, the promoters were cotransfected with overexpression plasmids for serum response factor and myocardin (Myocd). (A) normalized to pGL3basic no treatment, (B) normalized to each promoter no treatment, black bars indicate empty pGL3_basic vector, open bars Acta1 promoter and grey bars Acta2 promoter activity with no treatment (-) or 500 nM insulin stimulation or transfection without (wo) Myocd or dimethylsulfoxide (DMSO) treatment or 1 μM phorbol 12-myristate 13-acetate (PMA) stimulation, promoter firefly luciferase activities were normalized to SV40 renilla luciferase and presented as mean. n=2 for - and insulin, n=1 for wo Myocd, DMSO and PMA

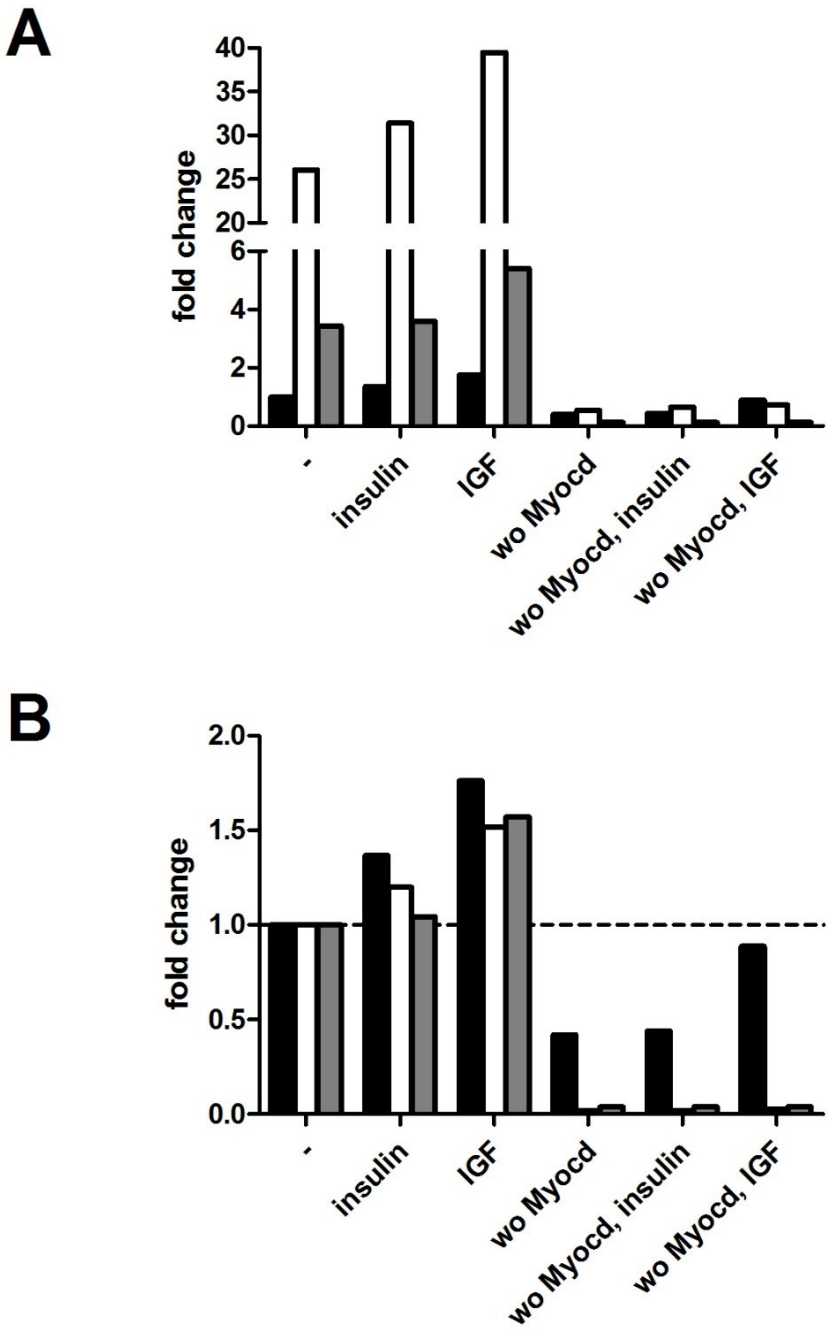

Figure 9. Empty pGL3_basic, skeletal muscle alpha actin (Acta1) and smooth muscle alpha actin (Acta2) promoter activities 24 hours after transfection into CHO-IR cells, the promoters were cotransfected with overexpression plasmids for serum response factor and myocardin (Myocd). (A) normalized to pGL3basic no treatment, (B) normalized to each promoter no treatment, black bars indicate empty pGL3_basic vector, open bars Acta1 promoter and grey bars Acta2 promoter activity with no treatment (-) or 500 nM insulin stimulation or 100 nM insulin-like growth factor 1 (IGF) stimulation or transfection without (wo) Myocd or wo Myocd or wo Myocd and insulin stimulation or wo Myocd and IGF stimulation, promoter firefly luciferase activities were normalized to CMV renilla luciferase and presented as mean. n=2 for pGL3_basic and Acta1 with -, insulin stimulation and wo Myocd, n=1 for everything else

7.9 Insulin stimulation had no effect on ERK and RSK phosphorylation in WT and cIR-IGFRdKO mice in both sexes

Figure 10 shows phosphorylated to total cardiac protein expression in insulin stimulated and control 9-week-old male cIR-IGFRdKO and WT mice, one week after knockout induction. The basal and insulin-induced levels of phophorylated Akt at Ser473 to total Akt protein were higher in WT compared to KO hearts. Insulin stimulation had no effect on phosphorylated ERK 1/2 at Thr202/Tyr204 to total ERK protein or phosphorylated p90RSK at Ser380 to total RSK protein.

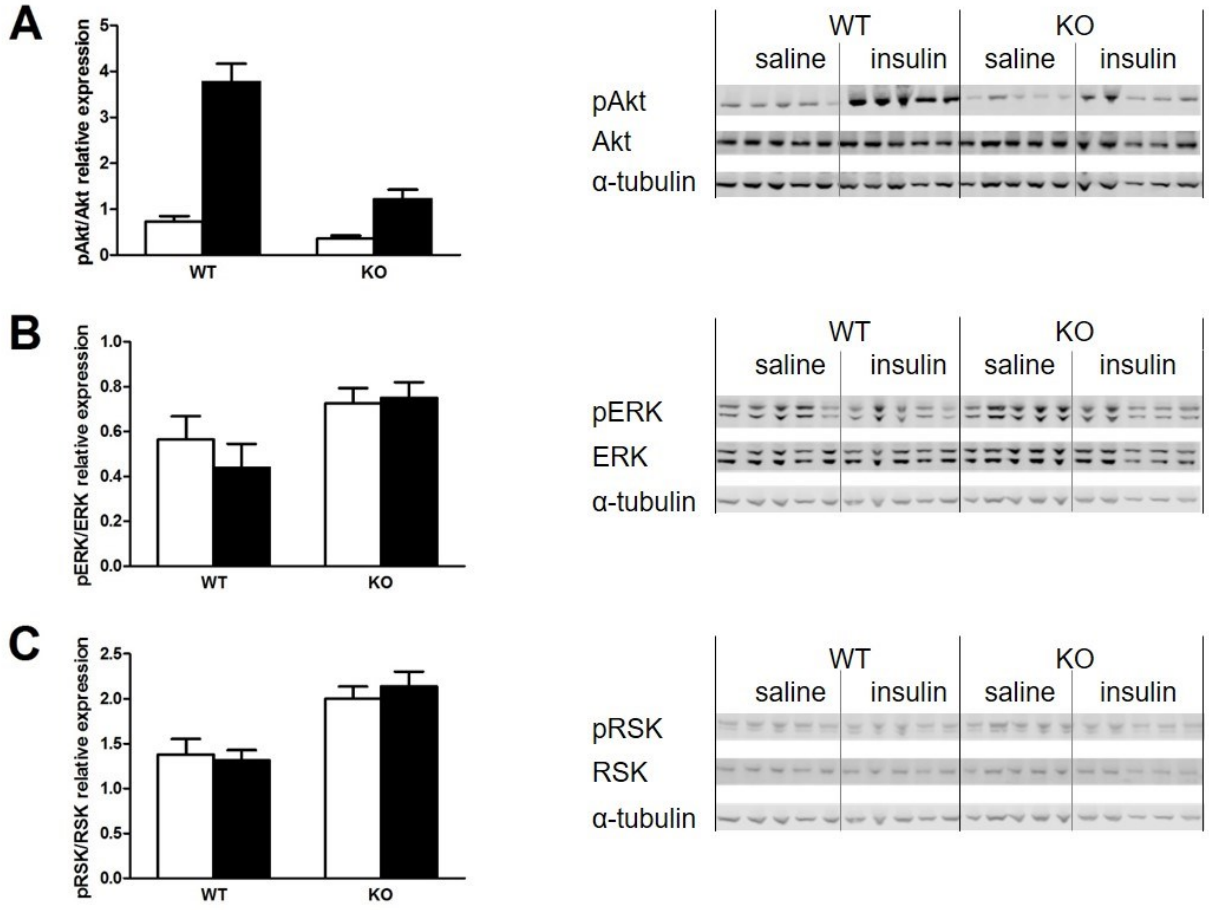

Figure 10. Cardiac protein expression in 9-week-old male cardiac inducible double knockout of insulin receptor and insulin-like growth factor 1 receptor (KO) and wildtype mice (WT), one week after knockout induction, after 10 minutes of insulin or saline injection into the inferior vena cava, open bars indicate saline treatment, black bars insulin treatment, (A) level of phophorylated Akt at Ser473 to total Akt protein, (B) level of phosphorylated ERK 1/2 at Thr202/Tyr204 to total ERK protein, (C) level of phosphorylated p90RSK at Ser380 to total RSK protein, values were normalized to α-tubulin and presented as mean ± standard deviation of mean. n=5

Figure 11 shows phosphorylated to total cardiac protein expression in insulin stimulated and control 9-week-old female cIR-IGFRdKO and WT mice, one week after knockout induction. Females obtained similar results as males. Insulin stimulation led to Akt phosphorylation, which was partly reduced in KO mice. However, insulin stimulation had no effect on phosphorylation from ERK or RSK.

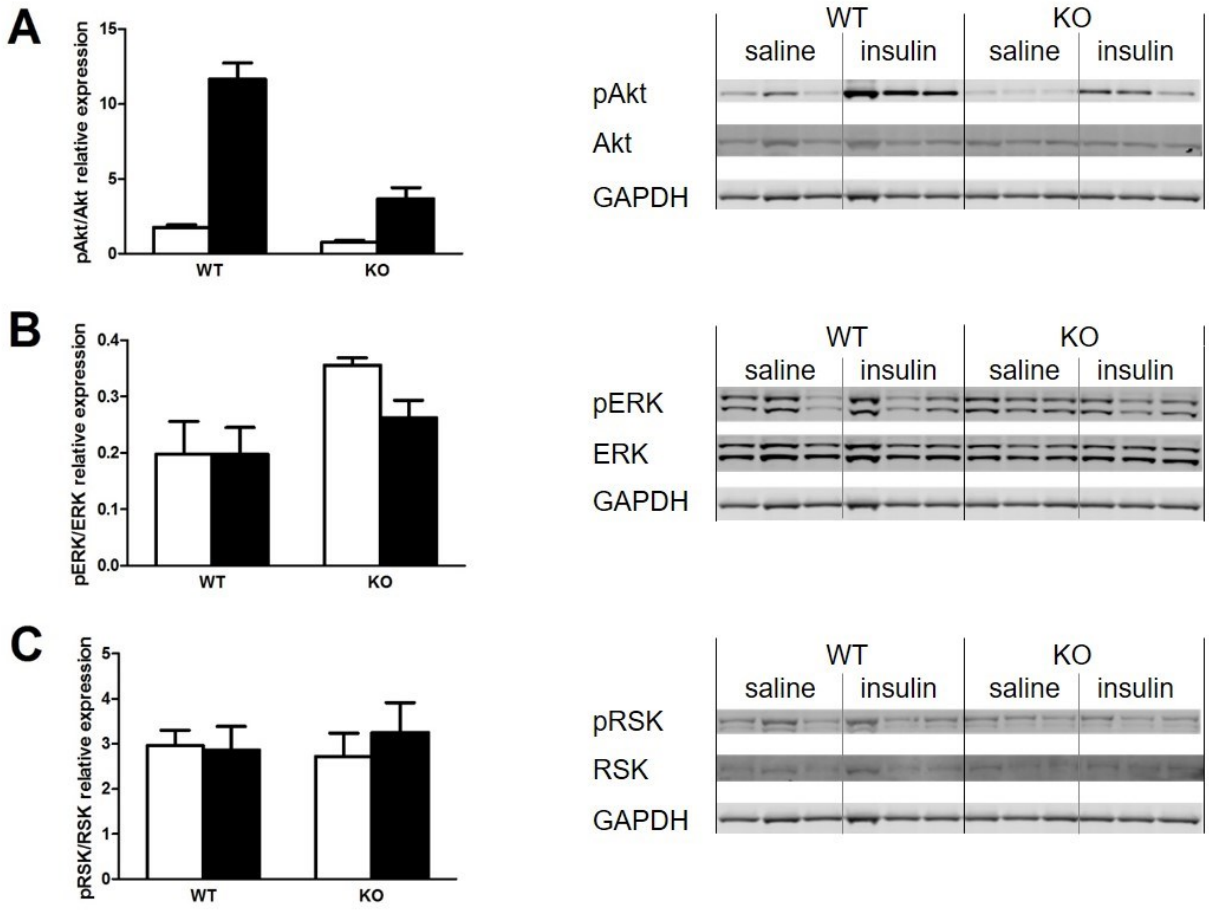

Figure 11. Cardiac protein expression in 9-week-old female cardiac inducible double knockout of insulin receptor and insulin-like growth factor 1 receptor (KO) and wildtype mice (WT), one week after knockout induction, after 10 minutes of insulin or saline injection into the inferior vena cava, open bars indicate saline treatment, black bars insulin treatment, (A) level of phophorylated Akt at Ser473 to total Akt protein, (B) level of phosphorylated ERK 1/2 at Thr202/Tyr204 to total ERK protein, (C) level of phosphorylated p90RSK at Ser380 to total RSK protein, values were normalized to GAPDH and presented as mean ± standard deviation of mean. n=3

8 Discussion

In the current study, mice with cardiac inducible double knockout of insulin receptor and insulin-like growth factor 1 receptor (cIR-IGFRdKO) presented with reduced heart weight and signs of heart failure. The biggest change in mRNA expression of sarcomeric proteins was observed with skeletal muscle alpha actin (Acta1) and smooth muscle alpha actin (Acta2). Expression of these genes was reduced in cIR-IGFRdKO mice and increased in insulin stimulated neonatal rat cardiomyocytes (NRCM). This lends support to the notion that insulin can regulate the expression of Acta1 and Acta2. Acta1 and Acta2 seem to be serum response factor (SRF) targets in a myocardin dependent manner. However, insulin stimulation does not seem to show a specific effect on Acta1 and Acta2 promoter activities through an SRF dependent mechanism.

Female cIR-IGFRdKO mice showed upregulation of atrial natriuretic peptide (ANP) as well as brain natriuretic peptide (BNP) coding genes one week after knockout induction, indicating heart failure development (Sergeeva und Christoffels 2013, Yoshimura et al. 2001). Previous studies have shown impaired cardiac function in transgenic mice lacking insulin receptor systemically. Mice with cardiac-specific knockout of insulin receptor showed reduced ejection fraction (Belke et al. 2002, Riehle et al. 2015). Combined deficiency of insulin receptor and IGF receptor in cardiac and skeletal muscle results in death from heart failure within the first month of life. In terms of cardiac function, insulin receptor seems to be more important than IGF receptor (Laustsen et al. 2007). Insulin signaling has been found to preserve contractile function by maintaining sarcomeric protein expression in the adult heart (Riehle et al. 2015).

We could show that female cIR-IGFRdKO mice showed a significant reduction in Acta1 mRNA expression one week after knockout induction. Expression levels of Acta2, gap junction protein and troponin T remained unchanged. In contrast to our results, Laustsen et al. described upregulation of Acta1 and troponin I in hearts from muscle-specific insulin receptor and IGF receptor knockout mice (Laustsen et al. 2007). These experiments were performed in a constitutive knockout model of muscle-specific insulin and IGF receptor. Therefore, insulin and IGF signaling were deleted from the beginning of life. Insulin signaling seems not to be necessary for prenatal growth and metabolic control in rodents, but for postnatal fuel homeostasis (Kitamura et al. 2003). Thus, the entire body adapts postnatally to systematic metabolic disturbances in a constitutive knockout model. These side effects can confound experimental results. Use of inducible and tissue-specific knockout models could be

advantageous to check specific roles of insulin signaling on adult cardiomyocyte`s function and metabolism.

Downregulation of several genes involved in cardiac structure has been described in cIR-IGFRdKO mice as well as in mice with cardiac inducible double knockout of insulin receptor substrates 1 and 2 (cIRSdKO) (Riehle et al. 2015). Besides other genes, Riehle et al. have found downregulation of Acta1, Acta2, gap junction protein and troponin T in cIR-IGFRdKO male mice. Differences to our results might be caused by different sexes of cIR-IGFRdKO mice or different time points of gene expression measurements after knockout induction. We used female cIR-IGFRdKO mice one week after knockout induction and Riehle et al. male cIR-IGFRdKO mice three days after knockout induction.

Conditional gene knockout methods are often used to model human diseases (Doetschman und Azhar 2012). cIR-IGFRdKO mice are a model for the cardiac effect of type 2 diabetes in patients. Naturally, humans do not have a knockout of insulin receptor, but type 2 diabetic patients are characterized by insulin resistance and relative insulin deficiency (American Diabetes Association 2009). Type 2 diabetic patients showed impaired autophosohorylation of insulin receptor from abdominal skeletal muscles (Maegawa et al. 1991), which is probably accompanied by intracellular insulin signaling deficiency. Gene expression profiling from skeletal muscle of patients with poorly controlled type 2 diabetes revealed downregulation of Acta1, Acta2, myosin heavy chain, troponin I and troponin T (Sreekumar et al. 2002). Altogether, these results match to the downregulation of several mRNAs coding for sarcomeric proteins in models lacking insulin signaling.

Riehle et al. revealed loss of sarcomeric integrity in electron micrographs from cIR-IGFRdKO and cIRSdKO mice (Riehle et al. 2015). Previous studies found similar results. Laustsen et al. described abnormalities in the organization of cardiac sarcomeres in muscle-specific insulin receptor and IGF receptor knockout mice (Laustsen et al. 2007). Electron micrographs of cardiomyocytes from diabetic rats revealed disruption of banding patterns and separation at intercalated disks. Insulin treatment was able to recover banding pattern and intercalated disks partially (Thompson 1988). Taken together, these models present similar results regarding sarcomeric disarray to the animals used in this work.

Sarcomeres are key components of cardiomyocytes and cardiomyocytes are main components of the heart. Therefore, they play a crucial role in determination of heart size. In this study, hearts from female and male cIR-IGFRdKO mice weighed 15% less than wildtype (WT) hearts. Similar results were found in comparable animal models. Significant reduction in heart

weight was shown in cardiac-specific insulin receptor knockout mice as well as muscle-specific insulin receptor and IGF receptor knockout mice (Belke et al. 2002, Laustsen et al. 2007). Insulin signaling has been described to play an important role in the regulation of cardiomyocytes size (Shioi et al. 2002). We assessed the effect of insulin stimulation on insulin signaling in cIR-IGFRdKO hearts. Basal and insulin-induced levels of phosphorylated to total Akt protein were reduced in cIR-IGFRdKO mice compared to WT. Stimulation of insulin receptor and IGF receptor is known to activate the PI3K/Akt pathway (Siddle 2011). Transgenic mice with cardiac overexpression of PI3K or Akt presented with larger hearts and increased cardiomyocyte cell size (Shioi et al. 2000, Condorelli et al. 2002). Furthermore, overexpression of Akt rescued the small cardiac phenotype from mice lacking cardiac insulin receptor (Shiojima et al. 2002). This suggests that reduced cardiac Akt phosphorylation in cIR-IGFRdKO mice might be a cause for reduced heart weight found.
We did not check which cell line contributed to the significant reduction in heart weight, but it is presumably due to cardiomyocytes since the KO is specific to that cell type. Laustsen et al. described reduced cardiomyocytes cell size without increased interstitial fibrosis in muscle-specific insulin receptor and IGF receptor knockout mice (Laustsen et al. 2007). Belke et al. described decreased cardiomyocyte areas, but no difference in cardiac collagen content in cardiac-specific insulin receptor knockout mice (Belke et al. 2002). Therefore, a significant reduction in heart weight from cIR-IGFRdKO mice may result from reduction in cardiomyocyte cell size. Downregulation of genes involved in cardiac structure potentially support this hypothesis. However, the effect of insulin signaling on regulation of sarcomeric protein expression is not known.

Insulin has been found to activate the mitogen activated protein kinases/extracellular signal-regulated kinases (MAPK/ERK) signaling cascade (Sutherland et al. 2013), which activates the phosphorylated 90 kDa ribosomal S6 kinase (p90RSK) through phosphorylation. MAPK/ERK cascade and RSK family are involved in cell growth related gene expression (Anjum und Blenis 2008). Thus, we measured insulin stimulated ERK1/2 and p90RSK phosphorylation in hearts of cIR-IGFRdKO mice. Insulin stimulation had no effect on cardiac phosphorylation of ERK1/2 and p90RSK. In contrast to our results, insulin-stimulated ERK1/2 phosphorylation has been shown in skeletal muscle (Rui et al. 2001), aortae (Symons et al. 2009), liver and fat of mice (Tomilov et al. 2011). Furthermore, insulin-mediated p90RSK phosphorylation was described in skeletal muscle of mice (Grzelkowska-Kowalczyk und Wieteska 2005). Higher ERK1/2 and p90RSK phosphorylation compared to our results could be due to tissue specific

differences in insulin signaling pathways. More likely, our insulin stimulation into the inferior vena cava of cIR-IGFRdKO mice might have been too short or our dose too low to activate the insulin signaling cascade fully. To address the ERK1/2 and p90RSK phosphorylation we used NRCM to evaluate the effect of insulin stimulation. In this study, insulin activated Akt, ERK1/2 and p90RSK by phosphorylation in NRCM. Other studies showed equivalent results regarding insulin-induced Akt phosphorylation (Mellor et al. 2014) as well as ERK1/2 phosphorylation in NRCM (Morisco et al. 2007).

As described above, loss of insulin signaling in adult cardiomyocytes of transgenic mice caused a decrease in mRNA expression levels of sarcomeric proteins. Accordingly, insulin stimulation in NRCM is likely to increase mRNA expression levels of sarcomeric proteins. We saw an upregulation of Acta1 and Acta2 mRNA expression in insulin stimulated NRCM. Previously, insulin and IGF have been suggested to regulate cardiac growth (DeBosch und Muslin 2008). Insulin and IGF may activate the MAPK/ERK as well as the PI3K/Akt pathway, which both stimulate protein synthesis and inhibit protein breakdown (Heineke und Molkentin 2006). Shiojima et al. saw an insulin-induced cardiomyocyte hypertrophy in NRCM (Shiojima et al. 2002). IGF stimulation induced hypertrophy in NRCM and increased mRNA levels for Acta1, myosin light chain and troponin I (Ito et al. 1993). Hence, our insulin administration on NRCM probably induced hypertrophy and growth-related upregulation of sarcomeric proteins. This is probably because of some indirect effect though since our promoter activity studies did not show activation.

We assessed the contribution of the MAPK/ERK signaling cascade in insulin-mediated regulation of sarcomeric protein expression. ERK inhibitor completely abolished insulin-induced ERK1/2 and p90RSK activation in NRCM. Similar results were obtained from other groups. Studies showed ERK1/2 inhibition through the same inhibitor in NRCM (Zhai et al. 2007, Ruppert et al. 2013). Furthermore, the same inhibitor abolished insulin-induced ERK1/2 phosphorylation and p90RSK activity in human skeletal muscle cells (Kotova et al. 2006).

In this study, insulin stimulation led to an increase in Acta1 and Acta2 mRNA expression. Inhibition of ERK blunted that increase. The tremendous effect of ERK inhibition on basal expression makes it difficult to interpret the data. It may be impossible to overcome that level of inhibition with any stimulus that would increase Acta1 or Acta2 expression. Therefore, the concentration of PD98059 may need to be titered to find a concentration that inhibits ERK activity but does not have such a profound effect on basal gene expression. However, experiments with ERK inhibitor in NRCM revealed that ERK1/2 is required for sarcomeric

organization after hypertrophy induction (Clerk et al. 1998). Ruppert et al. reported attenuation of phenylephrine induced cardiomyocyte hypertrophy by ERK inhibition (Ruppert et al. 2013). Further experiments with phenylephrine added as a positive control could aid in interpretation of the current results. The profound effect of ERK inhibition of basal expression of Acta1 and Acta2 does support the idea that MAPK/ERK signaling is an important regulator of cardiac hypertrophy and involved in sarcomeric integrity. Impaired cardiac insulin signaling in cIR-IGFRdKO mice might be a cause for sarcomeric disarray found. As mentioned above, MAPK/ERK cascade activates p90RSK which has been found to contribute to the transcriptional activation of SRF (Anjum und Blenis 2008). While we see evidence in both NRCMs and CHO-IR cells that insulin activates the MAPK/ERK to p90RSK pathway, activation of SRF remains murky.

SRF has been found to regulate the expression of contractile proteins required for proper assembly and function of cardiomyocytes. Besides Acta1 and Acta2, myosin heavy chains, myosin light chains, troponin C and troponin T were described as SRF targets (Miano et al. 2007). Cardiac-specific deletion of SRF in embryos results in lethal cardiac defects (Parlakian et al. 2004). Experiments with SRF-null neonatal cardiomyocytes revealed defects in the structure of the contractile apparatus in electron micrographs (Balza und Misra 2006). Consistent with the embryonic phenotypes, adult hearts lacking SRF show highly disorganized sarcomeres and rapid progression to heart failure (Parlakian et al. 2005). These studies showed similar phenotypes compared to cIR-IGFRdKO and cIRSdKO mice including sarcomeric disarray and heart failure. To test the hypothesis that lack of cardiac insulin signaling led to decreased SRF activity, followed by downregulation of several sarcomeric proteins, we measured Acta1 as well as Acta2 promoter activity. We overexpressed SRF and its transcriptional co-activator myocardin in a cell culture model, but did not find a specific effect of insulin stimulation on Acta1 or Acta2 promoter activity. The change that you see in Acta1 could be explained by a 2-fold induction in "activity" of promoter elements in the plasmid backbone. Even though, we overexpressed SRF and myocardin, experiments were performed in a heterologous cell system. Therefore our used CHO-IR cells might not have all of the transcriptional regulators that are present in cardiomyocytes. In contrast to our results, insulin stimulated a serum response element (SRE) luciferase reporter gene approximately nine fold in Chinese hamster ovary cells stably expressing high levels of insulin receptor (Yamauchi und Pessin 1994). SRE is the binding site for SRF in promoter regions of target genes and contains the CArG box sequence (Huet et al. 2005). The difference in insulin stimulated luciferase

reporter activity could be due to the portion of the sequence upstream of the promoter. We used a long promoter region from Acta1 as well as Acta2. Yamauchi et al. used a short promoter region of the c-fos gene (Yamauchi und Pessin 1994). Differences in length or promoter sequence, especially in the CArG box region, could have led to changes in SRF transcriptional activity.

It has been shown that in canine cardiac myoblasts insulin stimulation enhances SRF-SRE binding activity through activation of myocardin (Madonna et al. 2014). Insulin increased myocardin transcripts and protein levels, which may account for the activation of myocardin-dependent SRF-SRE binding (Madonna et al. 2014). In this study, transfections without myocardin led to markedly repressed Acta1, Acta2, and minimal promoter activity. Furthermore, insulin stimulation had no effect on promoter activities. Previously, it has been shown that myocardin is unable to activate SRF-dependent promoters in embryonic stem cells lacking SRF (Wang et al. 2002). Furthermore, transfection without myocardin did not activate SRF-dependent promoter regardless of increasing SRF amounts (Wang et al. 2001). These results highlight the importance of myocardin as co-activator of SRF. SRF can only bind to DNA and activate transcription in the presence of myocardin effectively (Du et al. 2003). We could show that transfection with SRF and myocardin led to highly increased activity of Acta1 promoter and increased activity of Acta2 promoter compared to a minimal promoter. In accordance with our results actin genes have been described as SRF target genes (Charvet et al. 2006, Miano et al. 2007, Parlakian et al. 2005, Zhang et al. 2001, Balza und Misra 2006). Gene microarray analysis from SRF-null neonatal cardiomyocytes revealed a huge decrease in Acta1 expression level and decrease in Acta2 expression level compared to control cardiomyocytes (Balza und Misra 2006). Based on the described expression levels and measured promoter activities, SRF seems to have a stronger influence on Acta1 gene expression than on Acta2 gene expression. However, we failed to demonstrate a specific induction in Acta1 and Acta2 promoter activity in response to insulin.

Limitations of the study

There are some limitations of this study. The first limitation concerns the low number of replicates and samples, especially in many of the transcription activity assays. Furthermore, experiments were performed in NRCM and CHO-IR cells to test a connection between insulin signaling and regulation of sarcomeric protein expression observed in adult mice

cardiomyocytes. Therefore, it is difficult to transfer results between these systems and conclusions are preliminary.

To determine if Acta1 and Acta2 promoter activities induced by insulin or IGF are generic or dependent on SRF alternative experiments could be performed. There are new luciferase constructs in which the half-life of the protein is greatly reduced. This gives a more accurate read out of transcriptional activity versus the steady state levels of mRNA and protein. Constructs could be made with the SRF sites in the Acta1 and Acta2 promoters mutated. Furthermore, SRF could be knocked down in NRCM and checked if the induction of Acta1 and Acta2 are reversed.

9 Conclusion

In the current study, mice with cardiac inducible double knockout of insulin receptor and insulin-like growth factor 1 receptor (cIR-IGFRdKO) presented with reduced heart weight and signs of heart failure. The biggest change in mRNA expression of sarcomeric proteins was observed with skeletal muscle alpha actin (Acta1) and smooth muscle alpha actin (Acta2). Expression of these genes was reduced in cIR-IGFRdKO mice and increased in insulin stimulated neonatal rat cardiomyocytes. This lends support to the notion that insulin can regulate the expression of Acta1 and Acta2. Acta1 and Acta2 seem to be serum response factor (SRF) targets in a myocardin dependent manner. However, insulin stimulation does not seem to show a specific effect on Acta1 and Acta2 promoter activities through an SRF dependent mechanism in in vitro transcription assays. The non-specific effect requires other approaches to definitively test our hypothesis.

Outlook

To investigate the connection between insulin signaling and regulation of sarcomeric protein expression in cardiomyocytes further studies could be conducted. Additional work could focus on the identification of insulin-dependent transcriptional programs that regulate sarcomeric integrity in adult hearts. One potential relevant family of transcription factors could be forkhead box O proteins. Forkhead box O proteins transcription factors have been shown as downstream targets of the insulin pathway involved in cardiac hypertrophy and could thus play an essential role in maintaining sarcomere structure and functional integrity in the adult heart.

10 Literature

Anjum R, Blenis J. 2008. The RSK family of kinases: emerging roles in cellular signalling. Nat Rev Mol Cell Biol, 9 (10):747-758.

Association AD. 2009. Diagnosis and Classification of Diabetes Mellitus. Diabetes Care, 32 (Suppl 1):S62-67.

Backer JM, Schroeder GG, Kahn CR, Myers MG, Jr., Wilden PA, Cahill DA, White MF. 1992. Insulin stimulation of phosphatidylinositol 3-kinase activity maps to insulin receptor regions required for endogenous substrate phosphorylation. J Biol Chem, 267 (2):1367-1374.

Balza RO, Jr., Misra RP. 2006. Role of the serum response factor in regulating contractile apparatus gene expression and sarcomeric integrity in cardiomyocytes. J Biol Chem, 281 (10):6498-6510.

Behrends JC, Bichofberger J, Deutzmann R, Ehmke H, Frings S, Grissmer S, Hoth M, Kurtz A, Leipziger J, Müller F, Pedain C, Rettig J, Wagner C, Wichmeyer E. 2010. Duale Reihe Physiologie.

Belke DD, Betuing S, Tuttle MJ, Graveleau C, Young ME, Pham M, Zhang D, Cooksey RC, McClain DA, Litwin SE, Taegtmeyer H, Severson D, Kahn CR, Abel ED. 2002. Insulin signaling coordinately regulates cardiac size, metabolism, and contractile protein isoform expression. The Journal of Clinical Investigation, 109 (5):629-639.

Bundesamt S. 2015. Causes of death by type of disease Wiesbaden: Statistisches Bundesamt.

Charvet C, Houbron C, Parlakian A, Giordani J, Lahoute C, Bertrand A, Sotiropoulos A, Renou L, Schmitt A, Melki J, Li Z, Daegelen D, Tuil D. 2006. New Role for Serum Response Factor in Postnatal Skeletal Muscle Growth and Regeneration via the Interleukin 4 and Insulin-Like Growth Factor 1 Pathways. Molecular and Cellular Biology, 26 (17):6664-6674.

Clerk A, Michael A, Sugden PH. 1998. Stimulation of the p38 Mitogen-activated Protein Kinase Pathway in Neonatal Rat Ventricular Myocytes by the G Protein–coupled Receptor Agonists, Endothelin-1 and Phenylephrine: A Role in Cardiac Myocyte Hypertrophy? The Journal of Cell Biology, 142 (2):523-535.

Condorelli G, Drusco A, Stassi G, Bellacosa A, Roncarati R, Iaccarino G, Russo MA, Gu Y, Dalton N, Chung C, Latronico MVG, Napoli C, Sadoshima J, Croce CM, Ross J. 2002. Akt induces enhanced myocardial contractility and cell size in vivo in transgenic mice. Proceedings of the National Academy of Sciences of the United States of America, 99 (19):12333-12338.

DeBosch BJ, Muslin AJ. 2008. Insulin Signaling Pathways and Cardiac Growth. Journal of molecular and cellular cardiology, 44 (5):855-864.

Dimitriadis G, Mitrou P, Lambadiari V, Maratou E, Raptis SA. 2011. Insulin effects in muscle and adipose tissue. Diabetes Research and Clinical Practice, 93:S52-S59.

Dixon DM, Choi J, El-Ghazali A, Park SY, Roos KP, Jordan MC, Fishbein MC, Comai L, Reddy S. 2015. Loss of muscleblind-like 1 results in cardiac pathology and persistence of embryonic splice isoforms. Sci Rep, 5:9042.

Doetschman T, Azhar M. 2012. Cardiac-Specific Inducible and Conditional Gene Targeting in Mice. Circ Res, 110 (11).

Du KL, Ip HS, Li J, Chen M, Dandre F, Yu W, Lu MM, Owens GK, Parmacek MS. 2003. Myocardin Is a Critical Serum Response Factor Cofactor in the Transcriptional Program Regulating Smooth Muscle Cell Differentiation. Mol Cell Biol, 23 (7):2425-2437.

Forbes MS, Sperelakis N. 1985. Intercalated discs of mammalian heart: a review of structure and function. Tissue Cell, 17 (5):605-648.

Grzelkowska-Kowalczyk K, Wieteska W. 2005. Changes of insulin-mediated protein kinases phosphorylation and the expression of IGFBP-3 in skeletal muscle of streptozotocin-diabetic mice. Pol J Vet Sci, 8 (3):231-240.

Hamdani N, Kooij V, van Dijk S, Merkus D, Paulus WJ, Remedios CD, Duncker DJ, Stienen GJ, van der Velden J. 2008. Sarcomeric dysfunction in heart failure. Cardiovasc Res, 77 (4):649-658.

Heineke J, Molkentin JD. 2006. Regulation of cardiac hypertrophy by intracellular signalling pathways. Nat Rev Mol Cell Biol, 7 (8):589-600.

Huet A, Parlakian A, Arnaud MC, Glandieres JM, Valat P, Fermandjian S, Paulin D, Alpert B, Zentz C. 2005. Mechanism of binding of serum response factor to serum response element. Febs j, 272 (12):3105-3119.

Hwang PM, Sykes BD. 2015. Targeting the sarcomere to correct muscle function. Nat Rev Drug Discov, 14 (5):313-328.

Ito H, Hiroe M, Hirata Y, Tsujino M, Adachi S, Shichiri M, Koike A, Nogami A, Marumo F. 1993. Insulin-like growth factor-I induces hypertrophy with enhanced expression of muscle specific genes in cultured rat cardiomyocytes. Circulation, 87 (5):1715-1721.

Kannel WB, Hjortland M, Castelli WP. 1974. Role of diabetes in congestive heart failure: The Framingham study. The American Journal of Cardiology, 34 (1):29-34.

Kitamura T, Kahn CR, Accili D. 2003. Insulin receptor knockout mice. Annu Rev Physiol, 65:313-332.

Kotova O, Al-Khalili L, Talia S, Hooke C, Fedorova OV, Bagrov AY, Chibalin AV. 2006. Cardiotonic Steroids Stimulate Glycogen Synthesis in Human Skeletal Muscle Cells via a Src- and ERK1/2-dependent Mechanism. Journal of Biological Chemistry, 281 (29):20085-20094.

Laustsen PG, Russell SJ, Cui L, Entingh-Pearsall A, Holzenberger M, Liao R, Kahn CR. 2007. Essential role of insulin and insulin-like growth factor 1 receptor signaling in cardiac development and function. Mol Cell Biol, 27 (5):1649-1664.

Lee J, Pilch PF. 1994. The insulin receptor: structure, function, and signaling. Am J Physiol, 266 (2 Pt 1):C319-334.

MacIver DH, Dayer MJ, Harrison AJ. 2013. A general theory of acute and chronic heart failure. Int J Cardiol, 165 (1):25-34.

Madonna R, Geng YJ, Bolli R, Rokosh G, Ferdinandy P, Patterson C, De Caterina R. 2014. Co-activation of nuclear factor-kappaB and myocardin/serum response factor conveys the hypertrophy signal of high insulin levels in cardiac myoblasts. J Biol Chem, 289 (28):19585-19598.

Maegawa H, Shigeta Y, Egawa K, Kobayashi M. 1991. Impaired autophosphorylation of insulin receptors from abdominal skeletal muscles in nonobese subjects with NIDDM. Diabetes, 40 (7):815-819.

Matsui T, Rosenzweig A. 2005. Convergent signal transduction pathways controlling cardiomyocyte survival and function: the role of PI 3-kinase and Akt. J Mol Cell Cardiol, 38 (1):63-71.

Mellor KM, Varma U, Stapleton DI, Delbridge LMD. 2014. Cardiomyocyte glycophagy is regulated by insulin and exposure to high extracellular glucose. American Journal of Physiology - Heart and Circulatory Physiology, 306 (8):H1240-H1245.

Miano JM, Long X, Fujiwara K. 2007. Serum response factor: master regulator of the actin cytoskeleton and contractile apparatus. American Journal of Physiology - Cell Physiology, 292 (1):C70-C81.

Morisco C, Marrone C, Trimarco V, Crispo S, Monti MG, Sadoshima J, Trimarco B. 2007. Insulin resistance affects the cytoprotective effect of insulin in cardiomyocytes through an impairment of MAPK phosphatase-1 expression. Cardiovascular Research, 76 (3):453-464.

Mounier C, Posner BI. 2006. Transcriptional regulation by insulin: from the receptor to the gene. Canadian Journal of Physiology and Pharmacology, 84 (7):713-724.

Muller-Wieland D, Knebel B, Avci H, Lehr S, Laudes M, Ristow M, Krone W, Kotzka J. 2001. Insulin-regulated transcription factors: molecular link between insulin resistance and cardiovascular risk factors. Int J Obes Relat Metab Disord, 25 Suppl 1:S35-37.

Mytas DZ, Stougiannos PN, Zairis MN, Foussas SG, Pyrgakis VN, Kyriazis IA. 2009. Diabetic myocardial disease: pathophysiology, early diagnosis and therapeutic options. J Diabetes Complications, 23 (4):273-282.

O'Brien RM, Streeper RS, Ayala JE, Stadelmaier BT, Hornbuckle LA. 2001. Insulin-regulated gene expression. Biochemical Society Transactions, 29 (4):552-558.

Parlakian A, Tuil D, Hamard G, Tavernier G, Hentzen D, Concordet JP, Paulin D, Li Z, Daegelen D. 2004. Targeted inactivation of serum response factor in the developing heart results in myocardial defects and embryonic lethality. Mol Cell Biol, 24 (12):5281-5289.

Parlakian A, Charvet C, Escoubet B, Mericskay M, Molkentin JD, Gary-Bobo G, De Windt LJ, Ludosky M-A, Paulin D, Daegelen D, Tuil D, Li Z. 2005. Temporally Controlled Onset of Dilated Cardiomyopathy Through Disruption of the SRF Gene in Adult Heart. Circulation, 112 (19):2930-2939.

Rassow J, Hauser K, Netzker R, Deutzmann R. 2008. Duale Reihe Biochemie.

Riehle C, Abel ED. 2016. Insulin Signaling and Heart Failure. Circ Res, 118 (7):1151-1169.

Riehle C, Weatherford ET, Abel ED. 2015. Insulin Signaling Preserves Contractile Function by Maintaining Sarcomeric Protein Expression in the Adult Heart Santa Fe, NM:

Rinderknecht E, Humbel RE. 1978. The amino acid sequence of human insulin-like growth factor I and its structural homology with proinsulin. J Biol Chem, 253 (8):2769-2776.

Rui L, Aguirre V, Kim JK, Shulman GI, Lee A, Corbould A, Dunaif A, White MF. 2001. Insulin/IGF-1 and TNF-α stimulate phosphorylation of IRS-1 at inhibitory Ser(307) via distinct pathways. Journal of Clinical Investigation, 107 (2):181-189.

Ruppert C, Deiss K, Herrmann S, Vidal M, Oezkur M, Gorski A, Weidemann F, Lohse MJ, Lorenz K. 2013. Interference with ERKThr188 phosphorylation impairs pathological but not physiological cardiac hypertrophy. Proceedings of the National Academy of Sciences, 110 (18):7440-7445.

Sergeeva IA, Christoffels VM. 2013. Regulation of expression of atrial and brain natriuretic peptide, biomarkers for heart development and disease. Biochimica et Biophysica Acta (BBA) - Molecular Basis of Disease, 1832 (12):2403-2413.

Shioi T, Kang PM, Douglas PS, Hampe J, Yballe CM, Lawitts J, Cantley LC, Izumo S. 2000. The conserved phosphoinositide 3-kinase pathway determines heart size in mice. The EMBO Journal, 19 (11):2537-2548.

Shioi T, McMullen JR, Kang PM, Douglas PS, Obata T, Franke TF, Cantley LC, Izumo S. 2002. Akt/Protein Kinase B Promotes Organ Growth in Transgenic Mice. Molecular and Cellular Biology, 22 (8):2799-2809.

Shiojima I, Yefremashvili M, Luo Z, Kureishi Y, Takahashi A, Tao J, Rosenzweig A, Kahn CR, Abel ED, Walsh K. 2002. Akt signaling mediates postnatal heart growth in response to insulin and nutritional status. J Biol Chem, 277 (40):37670-37677.

Siddle K. 2011. Signalling by insulin and IGF receptors: supporting acts and new players. J Mol Endocrinol, 47 (1):R1-10.

Sreekumar R, Halvatsiotis P, Schimke JC, Nair KS. 2002. Gene Expression Profile in Skeletal Muscle of Type 2 Diabetes and the Effect of Insulin Treatment. Diabetes, 51 (6):1913-1920.

Stanley WC, Chandler MP. 2002. Energy metabolism in the normal and failing heart: potential for therapeutic interventions. Heart Fail Rev, 7 (2):115-130.

Stanley WC, Recchia FA, Lopaschuk GD. 2005. Myocardial substrate metabolism in the normal and failing heart. Physiol Rev, 85 (3):1093-1129.

Sutherland C, O'Brien RM, Granner DK. 2013. Insulin Action Gene Regulation. Austin (TX): Madame Curie Bioscience Database.

Swan JW, Anker SD, Walton C, Godsland IF, Clark AL, Leyva F, Stevenson JC, Coats AJ. 1997. Insulin resistance in chronic heart failure: relation to severity and etiology of heart failure. J Am Coll Cardiol, 30 (2):527-532.

Symons JD, McMillin SL, Riehle C, Tanner J, Palionyte M, Hillas E, Jones D, Cooksey RC, Birnbaum MJ, McClain DA, Zhang Q-J, Gale D, Wilson LJ, Abel ED. 2009. Contribution of Insulin and Akt1 Signaling to Endothelial Nitric Oxide Synthase in the Regulation of Endothelial Function and Blood Pressure. Circulation Research, 104 (9):1085-1094.

Taha C, Klip A. 1999. The Insulin Signaling Pathway. The Journal of Membrane Biology, 169 (1):1-12.

Taylor R. 2012. Insulin Resistance and Type 2 Diabetes. Diabetes, 61 (4):778-779.

Thompson EW. 1988. Structural manifestations of diabetic cardiomyopathy in the rat and its reversal by insulin treatment. Am J Anat, 182 (3):270-282.

Tomilov AA, Ramsey JJ, Hagopian K, Giorgio M, Kim KM, Lam A, Migliaccio E, Lloyd KC, Berniakovich I, Prolla TA, Pelicci P, Cortopassi GA. 2011. The Shc locus regulates insulin signaling and adiposity in mammals. Aging cell, 10 (1):55-65.

Wang D-Z, Chang PS, Wang Z, Sutherland L, Richardson JA, Small E, Krieg PA, Olson EN. 2001. Activation of Cardiac Gene Expression by Myocardin, a Transcriptional Cofactor for Serum Response Factor. Cell, 105 (7):851-862.

Wang D-Z, Li S, Hockemeyer D, Sutherland L, Wang Z, Schratt G, Richardson JA, Nordheim A, Olson EN. 2002. Potentiation of serum response factor activity by a family of myocardin-related transcription factors. Proceedings of the National Academy of Sciences of the United States of America, 99 (23):14855-14860.

Yakar S. 2002. Circulating levels of IGF-1 directly regulate bone growth and density. J Clin Invest, 110 (6):771-781.

Yamauchi K, Pessin JE. 1994. Enhancement or inhibition of insulin signaling by insulin receptor substrate 1 is cell context dependent. Molecular and Cellular Biology, 14 (7):4427-4434.

Yao H, Han X, Han X. 2014. The cardioprotection of the insulin-mediated PI3K/Akt/mTOR signaling pathway. Am J Cardiovasc Drugs, 14 (6):433-442.

Yoshimura M, Yasue H, Ogawa H. 2001. Pathophysiological significance and clinical application of ANP and BNP in patients with heart failure. Can J Physiol Pharmacol, 79 (8):730-735.

Zhai P, Gao S, Holle E, Yu X, Yatani A, Wagner T, Sadoshima J. 2007. Glycogen synthase kinase-3alpha reduces cardiac growth and pressure overload-induced cardiac hypertrophy by inhibition of extracellular signal-regulated kinases. J Biol Chem, 282 (45):33181-33191.

Zhang W, Thompson BJ, Hietakangas V, Cohen SM. 2011. MAPK/ERK signaling regulates insulin sensitivity to control glucose metabolism in Drosophila. PLoS Genet, 7 (12):e1002429.

Zhang W, Elimban V, Nijjar MS, Gupta SK, Dhalla NS. 2003. Role of mitogen-activated protein kinase in cardiac hypertrophy and heart failure. Exp Clin Cardiol, 8 (4):173-183.

Zhang X, Azhar G, Chai J, Sheridan P, Nagano K, Brown T, Yang J, Khrapko K, Borras AM, Lawitts J, Misra RP, Wei JY. 2001. Cardiomyopathy in transgenic mice with cardiac-specific overexpression of serum response factor. American Journal of Physiology - Heart and Circulatory Physiology, 280 (4):H1782-H1792.

11 Appendix

11.1 Ehrenwörtliche Erklärung

Hiermit erkläre ich, dass mir die Promotionsordnung der Medizinischen Fakultät der FriedrichSchiller-Universität bekannt ist,

ich die Dissertation selbst angefertigt habe und alle von mir benutzten Hilfsmittel, persönlichen Mitteilungen und Quellen in meiner Arbeit angegeben sind,

mich folgende Personen bei der Auswahl und Auswertung des Materials sowie bei der Herstellung des Manuskripts unterstützt haben:

Eric T. Weatherford, PhD

Dr. rer. nat. Michael Schwarzer

die Hilfe eines Promotionsberaters nicht in Anspruch genommen wurde und dass Dritte weder unmittelbar noch mittelbar geldwerte Leistungen von mir für Arbeiten erhalten haben, die im Zusammenhang mit dem Inhalt der vorgelegten Dissertation stehen,

dass ich die Dissertation noch nicht als Prüfungsarbeit für eine staatliche oder andere wissenschaftliche Prüfung eingereicht habe und

dass ich die gleiche, eine in wesentlichen Teilen ähnliche oder eine andere Abhandlung nicht bei einer anderen Hochschule als Dissertation eingereicht habe.

Ort, Datum Unterschrift des Verfassers

11.2 Danksagung

An dieser Stelle möchte ich mich bei allen bedanken, die an der Entstehung meiner Dissertation mitgewirkt haben.

Ein besonderer Dank gilt Professor Torsten Doenst für die engagierte Unterstützung meiner Bewerbung für das Biomedical Exchange Program im Academic Year 2015/2016. Ohne diese wäre das Thema meiner Dissertation nicht zu Stande gekommen.

Herzlich bedanken möchte ich mich bei Professor Evan Dale Abel für die Möglichkeit meinen Forschungsaufenthalt in seinem Labor zu verbringen. Eric T. Weatherford, PhD, danke ich für die Überlassung des Promotionsprojektes und die umfassende Betreuung während der experimentellen Arbeit. Sein enormes Fachwissen und seine unerschütterliche Geduld waren sehr hilfreich im Labor. Ebenso danke ich Alec Seei, Trevor Funari und allen weiteren Abel Lab Mitarbeitern, die mich stets mit ihrem Wissen und ihrer Erfahrung unterstützt haben.

Weiterhin danke ich Dr. rer. nat. Michael Schwarzer für die kritische Betrachtung meiner Skripte und die Besprechungen dieser.

Ich danke meiner Familie und meinen Freunden für deren Unterstützung.

Nicht zuletzt möchte ich mich bei den Organisatoren des Biomedical Exchange Program und der finanziellen Unterstützung des Deutschen Akademischen Auslandsdienstes bedanken, die meinen Forschungsaufenthalt in Iowa City ermöglichten.